

POLITECNICO
MILANO 1863

School of Architecture Urban Planning
Construction Engineering

Master of Science in
Sustainable Architecture and Landscape Design

Solar Roofs for Kyiv's Khrushchevka Housing

Roof Design, Electrified Retrofit and District Energy Potential

Supervisor
Prof. Claudio Del Pero

Author
Oleksandra Bogdanenko
Student ID: 250058

Academic Year 2025–2026

Abstract

Rooftop photovoltaics can connect the renovation of Soviet-era housing with the expansion of local electricity generation. A representative five-storey residential building in Kyiv is examined in three long axis orientations: east–west, north–south and southeast–northwest. South-facing racks at 15° and 35° and an orientation-specific redesigned roof produce nine configurations.

Whole-module layouts establish installed capacity; PVGIS quantifies generation, while Ladybug radiation diagrams explain exposure and shading. The redesigned roofs produce 67.6–69.9 MWh/year. The east–west roof generates the most electricity, even tho 35° racks achieve the highest yield per installed kWp, they fit fewer modules.

A deep retrofit combines envelope improvements, efficient household appliances and heat pumps. Annual thermal demands are 67.5 MWh for heating, 14.3 MWh for cooling and 56.2 MWh for hot water. Hourly temperature-dependent conversion gives total electricity consumption of 97.1 MWh/year, including appliances, cooking and lighting, or 57.2 kWh/m²/year. East–west roof generation equals 72.1% of this annual demand. A separate historical household-electricity benchmark provides a second comparison. Across 63 residential roof units in Vidradnyi, adapted roof surfaces accommodate 12.6 MWp and produce an estimated 12.6 GWh/year. The annual and monthly comparisons show that redesigned roofs can supply a substantial share of retrofit electricity demand, with summer surpluses and winter shortfalls supporting the case for grid-connected collective generation.

Keywords: rooftop photovoltaics; Kyiv; Khrushchevka; roof retrofit; solar radiation; microdistrict; building electrification; collective solar generation.

Abstract in italian

Il fotovoltaico sulle coperture può collegare la riqualificazione dell'edilizia residenziale sovietica alla produzione locale di elettricità. Un edificio rappresentativo di cinque piani a Kyiv è analizzato con asse longitudinale est–ovest, nord–sud e sudest–nordovest. Per ogni orientamento si confrontano moduli rivolti a sud su supporti a 15° e 35° e una copertura riprogettata, per un totale di nove configurazioni.

Il posizionamento di moduli interi determina la potenza installata; PVGIS quantifica la produzione e i diagrammi Ladybug aiutano a interpretare esposizione e ombreggiamento. Le coperture riprogettate producono 67,6–69,9 MWh/anno. Il caso est–ovest offre la produzione maggiore, mentre i supporti a 35° hanno la resa specifica più alta ma ospitano meno moduli.

La riqualificazione profonda combina miglioramenti dell'involucro, elettrodomestici efficienti e pompe di calore. I fabbisogni termici annuali sono 67,5 MWh per il riscaldamento, 14,3 MWh per il raffrescamento e 56,2 MWh per l'acqua calda sanitaria. La conversione oraria in funzione della temperatura restituisce un consumo elettrico complessivo di 97,1 MWh/anno, inclusi elettrodomestici, cottura e illuminazione, pari a 57,2 kWh/m²/anno. La copertura est–ovest produce l'equivalente del 72,1% della domanda annuale. Un riferimento storico dei consumi elettrici domestici offre un secondo confronto. A Vidradnyi, 63 unità di copertura adattate ospitano 12,6 MWp e producono circa 12,6 GWh/anno. I confronti annuali e mensili mostrano che le coperture riprogettate possono soddisfare una quota significativa del fabbisogno elettrico dopo la riqualificazione, con eccedenze estive e deficit invernali che sostengono l'opportunità di una produzione collettiva connessa alla rete.

Parole chiave: fotovoltaico in copertura; Kyiv; Khrushchevka; riqualificazione delle coperture; radiazione solare; microdistretto; elettrificazione degli edifici; produzione solare collettiva.

Contents

Abstract 2
Abstract in italian 3
1 Introduction 8
1.1 The urban energy challenge 8
1.2 The solar city and the existing urban fabric 9
1.3 Research aims and architectural questions 9
1.4 How photovoltaic systems produce electricity 11
1.5 Architectural integration of rooftop photovoltaics 12
1.6 Advantages and limitations of roof retrofit 13
1.7 Incident solar radiation and the available resource 13
1.8 Solar geometry and shading 16
1.9 From the building comparison to the neighbourhood 17
2 Methodology 19
2.1 Approaches to urban solar potential assessment 19
2.2 From gross roof area to deployable capacity 20
2.3 Self-shading and the roof-packing trade-off 21
2.4 Research design and evidence sequence 22
2.5 Adapting a reference methodology 23
2.6 Boundaries adopted and not adopted 23
2.7 Geometric layout and row spacing 24
2.8 Calculation and reporting rules 24
2.9 Calculation workflow from geometry to results 25
3 Kyiv and the representative building 27
3.1 Energy resilience and the case for Kyiv 27
3.2 Existing solar research and the scale of inference 28
3.3 Electricity and heat in the residential context 28
3.4 Kyiv solar conditions in the adopted runs 29
3.5 Historical construction and archetype provenance 29
3.6 From historical plan to representative geometry 30
3.7 Final architectural configurations 31
4 Photovoltaic results and solar assessment 32
4.1 The adopted nine-case matrix 32
4.2 Verified annual generation 33
4.3 Tilt and azimuth input checks 33
4.4 Installed capacity and roof packing 34
4.5 Annual electricity generation 35
4.6 Specific yield and the tilt trade-off 36
4.7 Monthly generation for the north–south building 37
4.8 Monthly generation for the east–west building 38
4.9 Monthly generation for the southeast–northwest building 39
4.10 Monthly comparison of the redesigned roofs 40
4.11 Incident-radiation assessment 41
4.12 Radiation rose at 4.9° 42

4.13 Radiation rose at 15° ... 43
4.14 Radiation rose at 35° ... 44
4.15 Roof design and photovoltaic performance ... 44
5 Electricity demand and the electrified retrofit ... 46
5.1 Historical household electricity reference ... 46
5.2 Envelope, comfort and efficient appliances ... 47
5.3 Hourly thermal demand and heat-pump electricity ... 49
5.4 Thermal demand and internal heat gains ... 50
5.5 Annual and monthly electricity demand ... 53
5.6 PV generation relative to retrofit electricity ... 55
6 District rooftop PV potential and community energy ... 58
6.1 Study area and roof units ... 60
6.2 Adapting the roof strategy ... 61
6.3 Estimated electricity generation ... 62
6.4 Reading the spatial results ... 64
6.5 Seasonal supply and collective use ... 65
6.6 Spatial implications and storage ... 67
7 Conclusion ... 69
References ... 71
Appendix A Monthly PV source values ... 77
N–S monthly values ... 77
E–W monthly values ... 78
SE–NW monthly values ... 79
Appendix B Heat-pump conversion ... 80
Appendix C Incident radiation legend detail ... 83
Appendix D District roof schedules ... 84
Schedule D.1 Selected roof geometry and generation ... 84
Schedule D.2 Annual generation comparison ... 88
Appendix E Appliances and cooking ... 92

List of figures and graphs

Figure 1.1 From photovoltaic cell to building electricity 12
Figure 1.2 Direct-beam, diffuse and global horizontal irradiance 14
Figure 1.3 Radiation components on a tilted receiving surface 14
Figure 1.4 Irradiance and irradiation 15
Figure 1.5 Direct transmission, scattering and absorption in the atmosphere 16
Figure 1.6 Geometric sun paths at Kyiv's latitude, 50.455° N 17
Figure 3.1 Elevation of the five-storey, 30-apartment building, standard project 1-480A-31 29
Figure 3.2 Typical floor plan of standard project 1-480A-31 30
Figure 3.3 Final isometric presentation of the nine roof cases 31
Figure 4.1 Final top-view layouts 32
Figure 4.2 Installed capacity from the whole-module layouts 34
Figure 4.3 Annual modelled PV generation of the nine layouts, checked against the source exports 35
Figure 4.4 Annual specific yield using each case's PVGIS entered capacity 36
Figure 4.5 N–S monthly PV generation 37
Figure 4.6 E–W monthly PV generation 38
Figure 4.7 SE–NW monthly PV generation 39
Figure 4.8 Monthly generation of the three redesigned roofs 40
Figure 4.9 Ladybug annual incident-radiation comparison 41
Figure 4.10 Annual radiation rose at 4.9° 42
Figure 4.11 Annual radiation rose at 15° 43
Figure 4.12 Annual radiation rose at 35° 44
Figure 5.1 Effect of the efficient-appliance package on annual thermal demand 50
Figure 5.2 Monthly heating, cooling and hot-water thermal demand 51
Figure 5.3 Transmitted solar energy in the earlier diagnostic and the adopted retrofit 52
Figure 5.4 Annual electricity consumption by use 53
Figure 5.5 Annual electricity per square metre of conditioned reference area 54
Figure 5.6 Monthly electricity demand by use and east–west redesigned-roof PV generation 55
Figure 5.7 Annual PV generation relative to the common retrofit electricity demand 56
Figure 5.8 Monthly PV generation minus the common retrofit electricity demand 56
Figure 6.1 Location of the Vidradnyi study area within Kyiv 58
Figure 6.2 Vidradnyi study area in satellite imagery (above) and assessed roof-unit identifiers (below) 59
Figure 6.3 Measured long-axis bearings, clockwise from true north 60
Figure 6.4 Selected transverse roofs and PV facing directions 61
Figure 6.5 Estimated annual electricity generation per assessed roof unit 62
Figure 6.6 Annual PV productivity per installed kWp 64
Figure 6.7 Combined monthly generation from the selected roofs 65
Figure 6.8 Conceptual collective-energy arrangement 67
Figure B.1 Temperature-dependent performance before the 0.91 delivery allowance 80
Figure C.1 Common annual incident-radiation legend used for all nine configurations in Figure 4.9, from 0 to 1,400 kWh/m² 83

List of tables and schedules

Table 2.1 The evidence sequence connecting each stage of the method to its supporting material..... 22
Table 2.2 Scope retained from the reference methodology 23
Table 4.1 Nine-case PV comparison..... 33
Table 4.2 Tilt and azimuth values entered into PVGIS for each case..... 33
Table 5.1 Annual PV generation relative to the historical household-electricity benchmark..... 46
Table 5.2 Adopted retrofit assumptions..... 47
Table 5.3 Annual thermal demands and heat-gain diagnostics..... 50
Table 5.4 Monthly thermal demand (MWh)..... 51
Table 5.5 Annual electricity by end use and conditioned reference area..... 53
Table 5.6 Redesigned-roof generation relative to the common annual retrofit electricity demand..... 55
Table 6.1 Scope of the district assessment..... 58
Table 6.2 Combined generation from the 63 assessed roof units 62
Table 6.3 Options for organising the collective resource..... 65
Table A.1 N–S monthly PV generation (kWh) 77
Table A.2 E–W monthly PV generation (kWh) 78
Table A.3 SE–NW monthly PV generation (kWh)..... 79
Table B.1 Cooling EER interpolation points 81
Table B.2 Monthly electricity after conversion (MWh) 82
Schedule D.1 Selected roof geometry and generation..... 84
Schedule D.2 Annual generation comparison..... 88
Table E.1 Annual appliance and cooking electricity for the whole building..... 92

1 Introduction

1.1 The urban energy challenge

Why should buildings become energy producers as well as energy consumers? As cities grow, they concentrate residential, commercial, industrial and transport activity within relatively limited geographical areas, so their energy demand is inseparable from how the urban fabric itself is organised. The buildings in which people live, work and learn are not isolated objects: together they form a large, long-lived piece of infrastructure whose construction and day-to-day operation shape the energy system for decades after the last brick is laid.

Moving away from fossil fuels is one of the defining infrastructural challenges of this century. The Paris Agreement, adopted in 2015, set the objective of keeping global warming well below 2°C while pursuing efforts to limit it to 1.5°C above pre-industrial levels (UNFCCC, 2015). Within that wider challenge, the existing building stock is a particularly consequential field of intervention. In 2019, buildings accounted for 31% of global final energy demand. Buildings were also responsible for 21% of global greenhouse-gas emissions when emissions from their operation, electricity and heat supply, and the production of cement and steel for construction and refurbishment are included (IPCC, 2022).

Residential, commercial and public buildings consume energy for heating, cooling, ventilation, lighting, domestic hot water and electrical equipment, so reducing their energy use and carbon footprint is an essential part of any long-term decarbonisation strategy. Renovation improves the envelope and the efficiency of building services; renewable generation changes how the remaining demand is met. The two interventions are related but not interchangeable — installing photovoltaics does not itself reduce a building's heating load, and a more efficient building does not automatically generate the electricity it consumes.

Rooftop photovoltaic (PV) systems matter here precisely because they use surfaces the city has already built. A roof that has only ever provided enclosure and weather protection can also become a productive piece of energy infrastructure. That gives architecture a direct stake in the energy transition: a roof's dimensions, orientation, slope and internal organisation all decide how much generating surface can actually be installed on it. The architectural challenge is to design a roof layout that accommodates solar panels efficiently and makes the best use of the available sunlight resource.

1.2 The solar city and the existing urban fabric

Rather than treating photovoltaic installations as a scatter of independent projects, the "solar city" concept treats the urban building stock itself as potential energy-generating infrastructure. Individual rooftops stay physically separate, but their combined contribution can become significant at neighbourhood scale — which pulls energy technology into the same conversation as urban planning, ownership, investment and everyday building use.

Byrne and colleagues examine rooftop PV across Amsterdam, London, Munich, New York, Seoul and Tokyo, bringing market, financing and policy conditions into an infrastructure-scale assessment (Byrne et al., 2016). Their comparison shows why available roof area alone cannot establish deployment potential: investment and resident participation also need effective institutional arrangements. Those conditions inform the discussion of collective generation in Vidradnyi, without assuming that another city's targets or tariffs apply to Kyiv.

The Vauban district in Freiburg offers a complementary architectural precedent. Built on a former military site, it combined a requirement for low-energy construction with passive-house, plus-energy and solar-building strategies, alongside community participation, shared infrastructure and integrated transport planning (City of Freiburg, n.d.). Its relevance here is the relationship it draws between building performance and neighbourhood organisation — not a claim that Vauban's construction standards or energy balance can be transplanted wholesale into an existing Kyiv residential district.

Between them, these two cases suggest that a solar transition develops at the intersection of building design, energy efficiency, municipal planning and resident participation. In an established apartment block, the roof may be physically ready for PV while the decisions about access, financing and responsibility remain completely unresolved. A map of potential generation supports that planning conversation; it does not, by itself, describe an energy community that actually exists.

A representative building provides a starting point for testing roof interventions across comparable blocks. Vidradnyi connects this building-scale comparison to a defined group of residential roofs, whose dimensions and orientations are measured individually. The microdistrict tradition of repeated apartment buildings makes a coordinated intervention plausible, while differences between roofs require adaptation.

1.3 Research aims and architectural questions

Kyiv makes a compelling case for this investigation because the reconstruction and resilience of its energy infrastructure now intersect directly with the renovation of an extensive inherited residential fabric. Repeated Soviet-era apartment blocks give the

study a common architectural intervention to work with, while their varied positions and orientations across the city test whether a single roof solution can really be applied consistently.

The primary aim here is to assess how rooftop PV layout and roof redesign affect the electricity-generating potential of a representative five-storey residential building. The work connects a geometric model to quantified generation, and from there establishes the conditions under which the selected solutions could transfer to comparable neighbourhood buildings. That is a more specific task than estimating the whole city's rooftop potential: it asks the physical question of *why* one design accommodates more generating capacity than another.

Four research questions organise the work that follows:

RQ1 — Higher yield or more panels? Among the tested layouts, which produces more annual electricity within the available roof area: a configuration with higher yield per installed kilowatt-peak (kWp), or one that accommodates more modules?

RQ2 — How should the roof respond to orientation? For buildings of the same archetype with different long-axis orientations, how can roof inclination and the direction faced by the PV modules be adapted to increase annual electricity generation?

RQ3 — How does generation compare with demand? What proportion of the historical household and communal electricity benchmark, and of the fully electrified retrofit's annual electricity demand, is equivalent to the annual generation of the selected roof layouts?

RQ4 — From one building to a microdistrict? How can the roof strategy be adapted to the dimensions and orientations of the assessed residential roof units in Vidradnyi, and what is their combined annual PV generation potential?

Together, the first two questions make roof form and module placement part of the analysis, rather than assuming every rotated building carries the same installed capacity; the second two connect the geometric result back to demand and to the realistic limits of transferability.

The building comparison establishes installed capacity, annual generation, specific yield and monthly production for nine configurations. The demand assessment considers a separate electrified retrofit alongside a historical household-electricity reference. The district extension then adapts and compares the two continuous roof forms for 63 residential roof units, selecting the higher annual generation under common layout rules.

1.4 How photovoltaic systems produce electricity

A photovoltaic (PV) cell is a semiconductor device that absorbs light and converts part of its energy directly into electricity: absorbed photons transfer energy to charge carriers in the material, and the cell's internal structure separates and collects those charges so that a current can flow through an external circuit (U.S. Department of Energy, n.d.-a). Crystalline silicon is the technology represented in this project's PVGIS runs. The electricity generated can supply building appliances and services, including heat pumps for space heating and hot water.

Individual cells are wired together to form a module, and modules are combined into an array; protective layers and the module frame let the cells operate outdoors, while mounting structures connect the array to the building. The modules themselves produce direct current (DC); an inverter converts this into the alternating current (AC) used by building's electrical equipment and can be exported to the grid, with cabling, protection, metering and controls completing the installation (U.S. Department of Energy, n.d.-b, n.d.-c). This modular arrangement matters architecturally because installed capacity can be increased simply by adding whole modules wherever the roof allows it.

Nominal module power is a rating under standard test conditions, rather than a constant output throughout the year. The adopted LONGi Hi-MO X10 LR7-54HVH-505M module is rated at 505 Wp (LONGi, n.d.). The 132 modules positioned on the E–W and SE–NW redesigned roofs therefore provide 66.7 kWp, while the 137 modules on the N–S redesigned roof provide 69.2 kWp. Actual generation varies with incident solar radiation, module operating conditions and system losses. Installed capacity, expressed in kilowatt-peak (kWp), is the combined rated power of the PV modules under standard test conditions. Annual electricity generation, expressed in kilowatt-hours (kWh) or megawatt-hours (MWh), is the energy they produce over a year. Capacity describes the size of the installation, while annual generation also depends on sunlight availability, panel inclination and orientation, shading, temperature and system losses. A larger installed capacity therefore does not necessarily produce more electricity unless these conditions are also considered.

Conversion efficiency is the percentage of incident solar power — the sunlight reaching a panel's surface — that the panel converts into electricity under specified conditions. Specific yield is annual electrical energy per installed kWp. Annual roof generation equals installed capacity multiplied by specific yield. Module efficiency influences how much capacity can fit within the available roof area, so a larger array can generate more electricity even when its yield per installed kWp is lower. This distinction explains the comparison between the 35° racks, 15° racks and redesigned roof surfaces in Chapter 4.

PVGIS combines the solar resource with a technology model and a system-performance calculation in a single step (European Commission Joint Research Centre, n.d.-a). Its resulting electricity estimate should not be multiplied by a second, generic efficiency or loss factor once those effects are already built in — and, in the other direction, a map of incident radiation alone is not an electricity calculation. Incident-radiation maps describe solar exposure, while the PVGIS outputs quantify electrical generation.

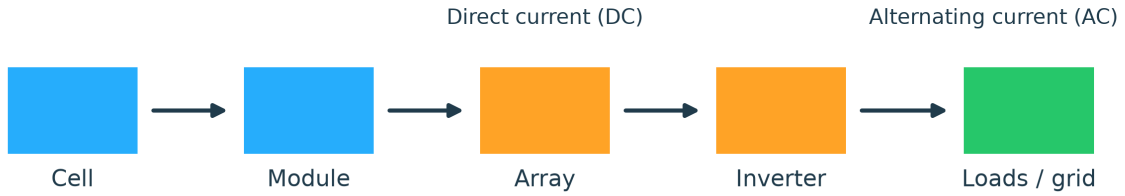

Figure 1.1 From photovoltaic cell to building electricity. Original schematic based on U.S. Department of Energy (n.d.-a–c).

1.5 Architectural integration of rooftop photovoltaics

Rooftop PV can be added onto an existing roof, or built directly into a building component. Building-Applied Photovoltaics (BAPV) sit on top of the building while the underlying envelope continues to do its original job; Building-Integrated Photovoltaics (BIPV) themselves fulfil a building function, such as replacing part of the roof covering outright. The distinction is about the construction role the product plays, not simply whether the modules happen to follow an architecturally designed slope (IEA PVPS Task 15, 2018).

On an existing flat roof, tilted racks let the modules be oriented independently of the building's own long axis. That flexibility comes at a cost: supports, clearances and spacing between rows all take from the usable area. A redesigned, inclined roof offers a more continuous surface instead, and can make the PV array part of the overall roof composition. Whether that surface ultimately counts as BAPV or BIPV depends on the specified assembly — waterproofing, support, replacement arrangements — and this research establishes the geometry and energy performance of that surface; it does not claim a complete, certified BIPV construction system.

The project therefore uses the term *redesigned roof with PV* for its three new roof configurations. The same representative building is studied with east–west, north–south and southeast–northwest long axes, with the roof geometry responding to each orientation while module rating and the core comparison assumptions stay consistent across all three. Architectural integration is judged here through the amount and

arrangement of solar-active surface achieved — not through an unsupported claim that every roof form is structurally or economically equivalent to every other.

1.6 Advantages and limitations of roof retrofit

Rooftop PV is modular, scalable and decentralised. It generates electricity close to the buildings that use it, and it can be introduced building by building or through a coordinated programme across several roofs at once. For an existing residential district, this lets the roofscape take on an additional function without needing a separate ground-level site for the array — and the design opportunity is strongest when energy generation is considered alongside access, maintenance and the building's future renovation.

The available roof area is also a hard physical limit. In a multi-storey apartment block, the roof does not grow in proportion to the dwellings beneath it, which is exactly why the roof-to-demand relationship studied by Aste and colleagues remains relevant even once a large share of the roof is already carrying modules (Aste et al., 2024). Adding modules can improve total generation, but it never removes the prior question of which electrical uses are actually being compared against it.

Installation also depends on the condition and capacity of the existing structure, its weatherproofing, wind and snow loading, drainage, maintenance access and equipment placement — constraints that should inform the available area before modules are ever counted. Geometric feasibility, in other words, is only the first level of assessment: a roof that fits an array in a model still needs building-specific structural and electrical design before anything is built. Project economics depend just as heavily on installation cost, financing, tariffs, operating arrangements and the timing of electricity use — these require a separate feasibility assessment beyond annual generation.

Distributed generation can support resilience, but a grid-connected PV array does not automatically keep a building powered during an outage: backup operation needs its own equipment, controls and an arrangement that can operate safely once the main grid disappears. Storage can extend generation's usefulness beyond daylight hours, but its energy and power ratings have to be matched against real load and generation data (U.S. Department of Energy, n.d.-d). Annual generation alone cannot determine a battery size or demonstrate backup operation.

1.7 Incident solar radiation and the available resource

Global horizontal irradiance (GHI) is the solar power received per unit area of horizontal surface. Direct normal irradiance (DNI) measures the direct beam on a surface perpendicular to the sun's rays; diffuse horizontal irradiance (DHI) measures scattered sky radiation on a horizontal surface. The direct beam must be projected onto

the horizontal plane before it is added to DHI: GHI = DNI · cos θz + DHI, where θz is the solar zenith angle (Sengupta et al., 2024).

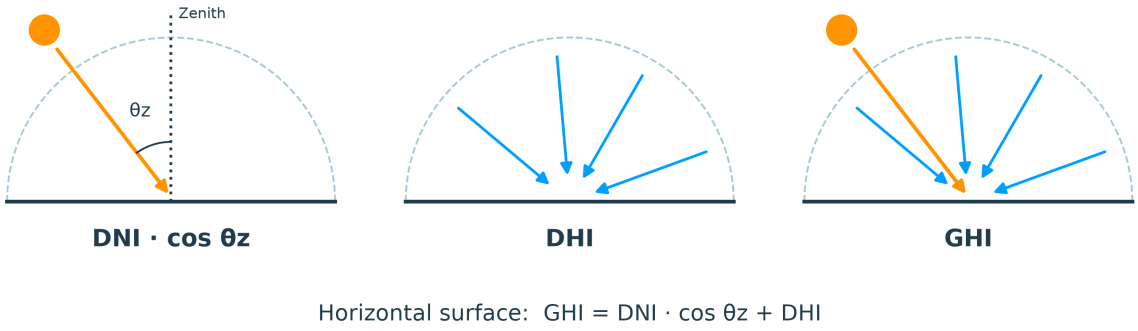

Figure 1.2 Direct-beam projection, diffuse radiation and global horizontal irradiance. θz denotes solar zenith angle. Original schematic based on Sengupta et al. (2024), Figure 2-7.

For a tilted module, the relevant quantity becomes *plane-of-array (POA) irradiance*: the beam contribution on that plane, plus diffuse sky radiation, plus radiation reflected off the ground or surrounding surfaces (Sandia National Laboratories, n.d.). Changing a module's tilt and azimuth therefore does more than change its instantaneous relationship to the sun — it changes the radiation received across the whole range of sky and sun conditions over the analysis period.

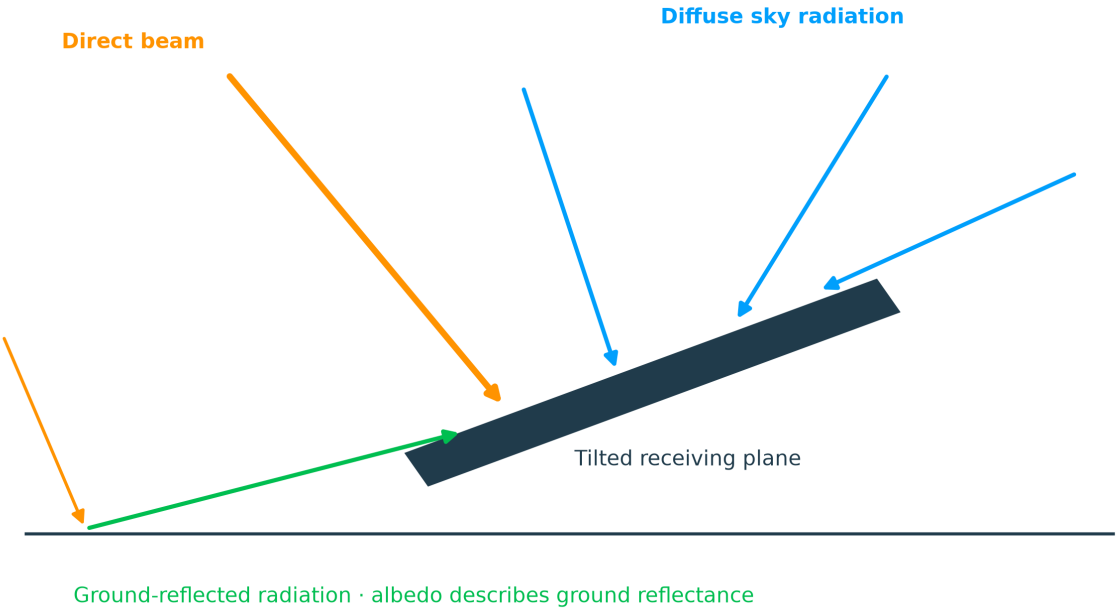

Figure 1.3 Direct, sky-diffuse and ground-reflected contributions on a tilted receiving surface. Original schematic informed by Bham et al. (2025) and Sandia National Laboratories (n.d.).

Irradiance describes the solar power reaching a surface at a given moment, expressed in watts per square metre (W/m²). Irradiation is the total solar energy received over a

specified period, such as an hour, a day or a year, expressed in Wh/m² or kWh/m². For example, a constant irradiance of 500 W/m² over two hours gives an irradiation of 1 kWh/m².

Integrating an irradiance curve over time gives the irradiation received during that period (NABCEP, 2019). The annual Ladybug diagrams and radiation roses show irradiation per unit area. Electrical generation additionally depends on module conversion and system losses.

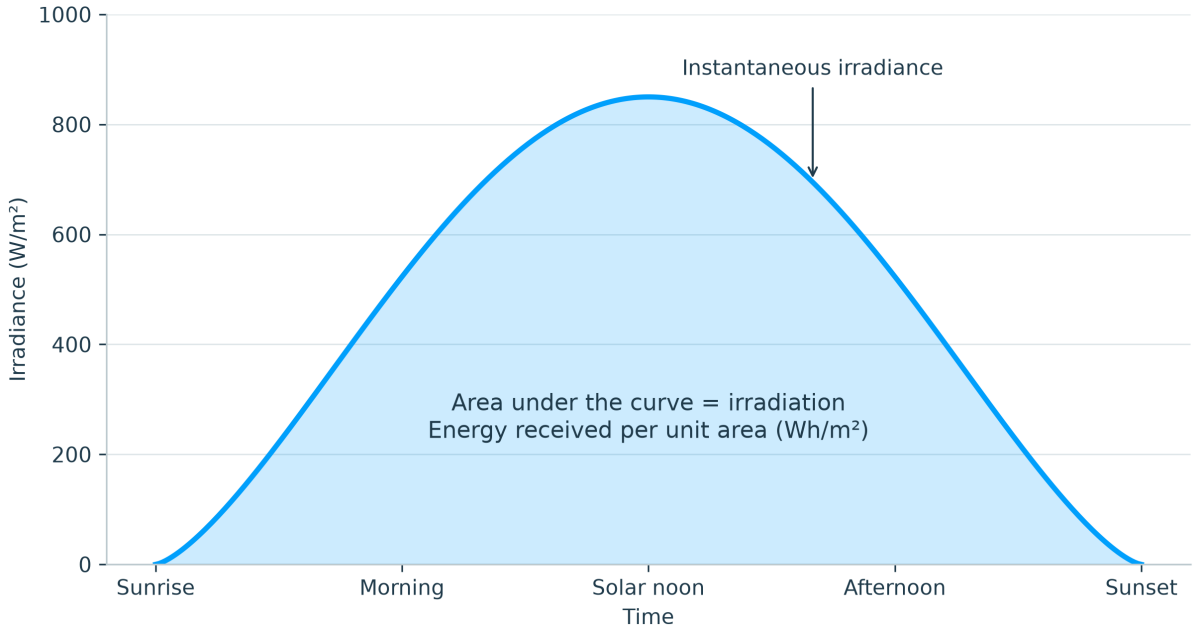

Figure 1.4 Irradiance is instantaneous power per unit area; the area under its time curve gives irradiation. Illustrative curve, not Kyiv weather data. Original diagram based on NABCEP (2019), Figure 30.

Clouds and atmospheric particles scatter and absorb sunlight, changing both the amount received at the ground and its division into direct and diffuse components. Modules continue to receive diffuse radiation even when the sun is obscured. The balance varies with weather, so no single diffuse fraction is assigned to Kyiv (Sengupta et al., 2024).

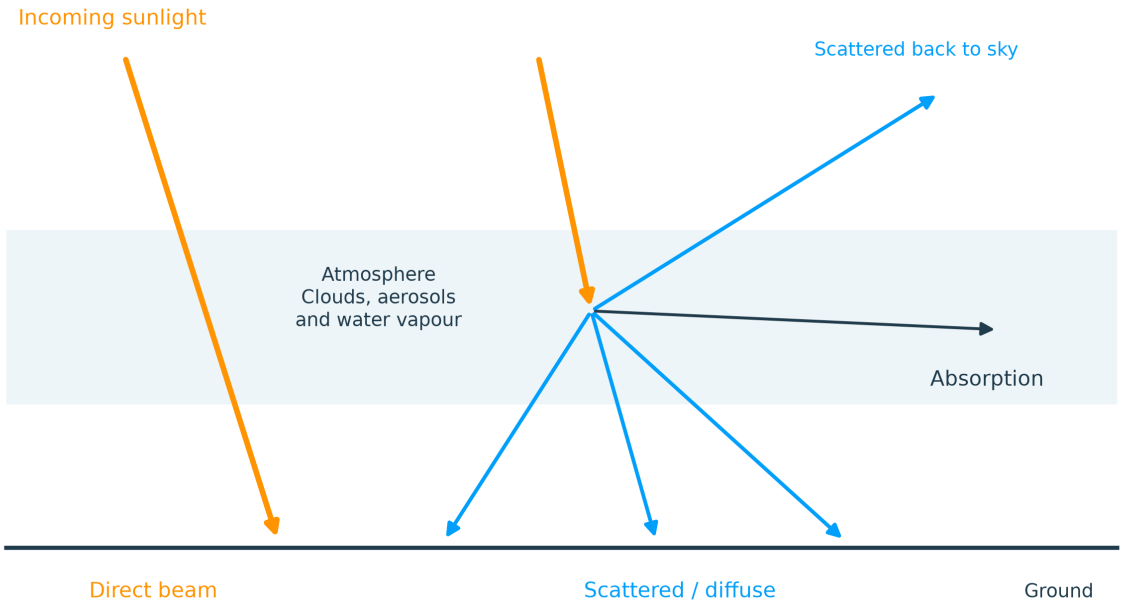

Figure 1.5 Direct transmission, scattering and absorption in the atmosphere. Arrows indicate pathways, not energy fractions. Original schematic based on Sengupta et al. (2024), Figure 2-5.

1.8 Solar geometry and shading

Solar altitude describes how high the sun is above the horizon, while solar azimuth describes its compass direction. For solar panels, azimuth instead describes the direction they face. Different tools express this direction using different starting points: PVGIS measures from south, while the mapping in Chapter 6 measures clockwise from north. A southeast-facing panel therefore has an azimuth of −45° in PVGIS and a bearing of 135° on the map. These values describe the same orientation.

Sun-path diagrams plot the sun's position through the year, and let the angular outline of an obstruction be compared directly against that path — useful for working out when a parapet, an adjoining building or another rooftop object might interrupt direct sunlight. At low solar altitudes, a given obstacle casts a longer shadow on a horizontal surface, which is why winter conditions matter so much for row-spacing decisions. But an unshaded winter location is not automatically unshaded all year round: the sun's azimuth keeps changing too, and different obstructions can affect its summer or shoulder-season path.

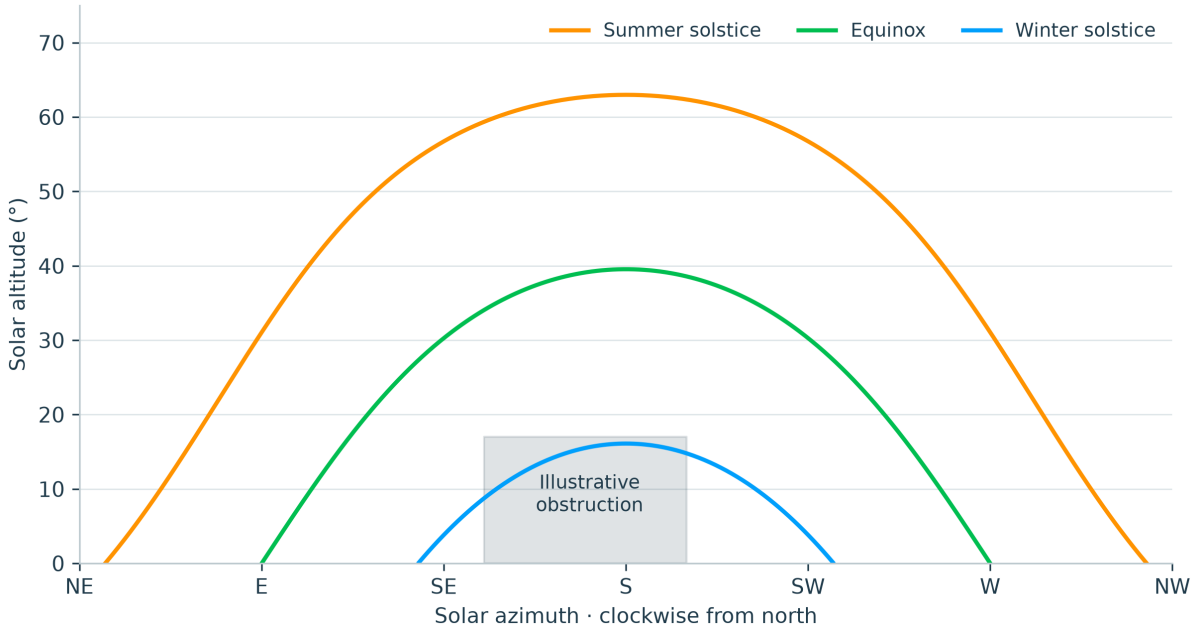

Figure 1.6 Geometric sun paths at Kyiv's latitude (50.5° N) for the summer solstice, equinoxes and winter solstice. The shaded rectangle illustrates a hypothetical obstruction; local terrain and atmospheric refraction are not represented. Calculated from standard solar geometry (NOAA, n.d.).

For a rooftop array, shading can come from the terrain, neighbouring buildings, rooftop enclosures, or simply the next row of modules. A distant terrain horizon and the local roof geometry sit at different scales of obstruction. This project uses PVGIS for quantitative generation and Ladybug for a spatial reading of the modelled roof context. The radiation images show where shading reduces the sunlight reaching the roof. Quantifying the resulting electricity loss would require a separate comparison of PV generation with and without shading under the same weather conditions.

The tilt with the highest annual yield per installed kWp may leave too little space for modules to maximise total roof generation. Steeper racks need greater row separation; shallower arrays can fit more capacity into the same footprint. The nine layouts test this trade-off with whole-module placement.

1.9 From the building comparison to the neighbourhood

The nine configurations establish the relation between roof form, orientation and module capacity. In Vidradnyi, the continuous roof strategies are adapted to each residential roof's measured length, width and direction. Both longitudinal and transverse slopes are compared under common rules, producing one selected generation scenario for the assessed roofs.

Transfer depends on roof dimensions, feasible rise, perimeter clearances and space for services. The selected residential roof units remain identifiable on the maps; other buildings are retained as context and excluded from the generation total.

The following chapters develop the calculation methods, the Kyiv building context, the nine-case PV comparison, the electrified retrofit and the Vidradnyi application.

2 Methodology

2.1 Approaches to urban solar potential assessment

Assessing urban solar potential involves estimating how much solar energy can be captured from the available building surfaces. The method depends on the purpose of the assessment, the available data and the scale of analysis. National assessments provide broad estimates, neighbourhood inventories identify suitable buildings and roof areas, and detailed layouts establish how many modules can fit on a particular roof. Although each approach may report installed capacity or annual electricity generation, the results reflect different levels of detail and should be interpreted accordingly.

Statistical, top-down approaches start from aggregate building stock information — dwelling counts, floor areas, or average roof areas by building type. They are well suited to screening large territories with limited data, but an average cannot resolve the orientation, obstacles or layout of an individual roof: this kind of estimate can establish the scale of an opportunity without saying where a single module could actually be placed.

GIS-based approaches keep the spatial identity of individual buildings. Footprints, land use, heights and roof attributes can be combined to classify candidate installation surfaces and aggregate the results. A footprint layer is a starting point rather than a complete roof model — it can omit equipment and roof slopes, and both its completeness and its positional accuracy need checking before use. The Vidradnyi assessment therefore retains separate roof-unit identifiers and documented geometric assumptions.

Three-dimensional radiation analysis shows how surrounding buildings and rooftop features affect the sunlight reaching a surface, including how shadows change with the sun's position. Freitas et al. (2015) highlight the importance of representing urban geometry while balancing spatial detail against computation time. This supports the use of detailed radiation analysis to compare roof layouts in Chapter 4, alongside a simpler method for assessing many roofs across Vidradnyi in Chapter 6.

Satellite imagery and machine-learning methods can help obtain building footprints or identify roof characteristics where cadastral data is incomplete, but they do not remove the need for geometry checks, and they are not a substitute for a PV conversion model. The national Ukrainian study discussed in Chapter 3 combines satellite-derived inputs, calibrated translation factors and energy modelling (Winkler et al., 2025); The neural network identifies roof geometry from imagery, while a separate

calculation estimates PV electricity generation using solar-resource data and assumptions about the installation.

The building comparison comprises nine PV configurations: three roof layouts for each of three building orientations. Hourly thermal calculations estimate heating, cooling and hot-water demand for the proposed retrofit, including the reduced internal heat gains from efficient appliances. These demands are then converted into electricity consumption using temperature-dependent heat-pump performance. At microdistrict scale, a QGIS inventory records the dimensions and orientations of 63 residential roof units in Vidradnyi, which inform roof layouts and PVGIS generation estimates. Both PV assessments use the same module specifications and common performance assumptions.

2.2 From gross roof area to deployable capacity

A defining step in any urban PV assessment is the translation from a large, theoretical roof resource to the surface that can actually support an installation. The study treats that translation as a sequence of explicit questions rather than a fixed set of universal percentages, because two assessments of the same territory can differ substantially depending on which surfaces they count and which constraints they apply — and a percentage borrowed from elsewhere hides that difference instead of resolving it.

The first quantity is the building footprint, measured as a horizontal projection. This does not necessarily equal the actual roof surface area: a pitched surface has a larger area than its footprint, and several roof planes can occupy one footprint. Usable installation area is narrower again, once access routes, equipment, roof openings, edge clearances and unsuitable portions have been excluded. Any method used here has to state plainly whether it is measuring horizontal area, inclined surface area, or module area, since the three give different numbers for the same roof.

Geometric and exposure constraints can be mapped or modelled directly. Structural capacity, fire access and construction feasibility, by contrast, require evidence specific to the building and the proposed intervention. A visually clear roof area is therefore a candidate installation surface, not a structural approval — and a building of unknown condition should be recorded as unknown, not folded into either the suitable or the unsuitable category.

Economic feasibility introduces a further boundary that the study does not attempt to examine. Expected generation has to be weighed against construction and operating costs, financing, and the value of electricity at the times it is used or exported; ownership, consent, heritage protection and grid-connection arrangements can limit implementation further. These questions are what separate theoretical, technical,

economic and achievable potential from one another - the estimates are not adjusted for costs or ownership constraints, which would need to be assessed for each building.

After defining the usable roof area, whole modules were arranged and counted within the adopted layout constraints. The layouts accounted for roof boundaries, excluded areas, gaps between modules and spacing between tilted rows. Residual spaces that could not accommodate a whole module remained unused. No additional roof-utilisation factor was applied, because these limitations were already reflected in the module count.

In Chapter 6, the roof strategy was applied to the 63 assessed residential roof units in Vidradnyi. Each roof's dimensions and orientation, together with the adopted setbacks and module spacing, determined the number of modules that could fit. Installed capacity was calculated from this module count and the rated power per module, while PVGIS estimated electricity generation for the selected inclination and facing direction.

2.3 Self-shading and the roof-packing trade-off

Tilted modules on a flat roof cast shadows onto the space behind them. Increasing tilt raises the upper edge of each row and increases the clearance needed to keep the row behind it unshaded; a lower solar altitude lengthens that shadow further. The final spacing choice therefore depends on tilt, row direction, the solar positions considered, and the amount of shading judged tolerable — not on latitude alone.

A ground coverage ratio (GCR) can describe how densely a row arrangement is packed, but its numerator has to be stated. Module surface area divided by the ground area assigned to an array is not the same quantity as the horizontal projection of those modules divided by that same area, and neither should be confused with the fraction of the whole roof remaining after access and equipment exclusions. Rather than assert an unsupported universal GCR for Kyiv, the study works directly from the documented module counts of the nine tested configurations.

A sloped roof lets modules follow a continuous plane without the repeated raised-row gaps a rack installation needs. It still requires a mounting or integration system, access, weatherproofing and a verified support structure of its own — redesigning the roof can increase generating capacity, but the energy comparison alone cannot establish that the new construction is the preferred structural or financial solution.

The controlled comparison in the analysis tests the architectural consequences of exactly these choices. The 15° and 35° rack cases isolate two tilt-and-packing arrangements on the existing flat roof; the redesigned cases explore a continuous solar-active surface adapted to each building's own axis. The roof configurations were

optimised for the reference building, considering its orientation, available dimensions, module arrangement and adopted design constraints.

2.4 Research design and evidence sequence

The method comprises five stages: geometry, solar exposure, electricity generation, electricity demand and district application. One representative building is assessed in three long-axis orientations and three roof configurations. Location, module rating, radiation database, PV technology and loss assumptions are held constant across the nine PVGIS cases. Installed capacity, tilt and azimuth vary with the configuration; module counts are established separately for each roof layout.

The analysis began by defining the representative building and its roof constraints, then arranging and counting modules for the nine configurations. Each layout established the installed capacity, panel inclination and facing direction. Ladybug radiation analysis showed differences in solar exposure, while the corresponding PVGIS calculations provided annual and monthly electricity generation. Generation was then compared with the historical electricity benchmark and the electrified retrofit demand. Finally, the roof strategy was adapted to the dimensions and orientations of the assessed buildings in Vidradnyi. This sequence linked the generation estimates to the roof geometry and module counts at both scales.

Table 2.1 The evidence sequence connecting each stage of the method to its supporting material.

Stage	**Evidence and output**
Archetype	Historical drawings, calculation notes and the latest model summary; traced geometry and use (Chapter 3).
Layout	Drawings of the nine roof configurations and module-count schedule; whole 505 W modules counted per case.
Radiation	Completed Ladybug plates and radiation roses; spatial exposure and local-context interpretation.
PV electricity	Nine matching PVGIS summaries; annual, monthly and specific-yield results.
Demand	Historical household benchmark; household-based efficient-appliance estimate; hourly thermal simulation and heat-pump electricity conversion.
GIS and REC	63 measured residential roof units in Vidradnyi; adapted layouts, PVGIS generation and collective-use interpretation.

2.5 Adapting a reference methodology

The reference-building comparison follows the approach of Aste et al. (2024): compare roof alternatives, count deployable photovoltaic capacity and relate generation to a defined electricity demand. Heating and cooling electricity are derived from hourly thermal loads using temperature-dependent heat-pump performance. The Kyiv application combines this approach with a household-based estimate of efficient appliances and electric cooking.

The adaptation, however, is substantial rather than a direct transposition. Aste et al. examine four European climates and a documented high-performance reference building; this study works with one Kyiv location and a Soviet-era five-storey Khrushchevka archetype instead. Their study assumes a constant installed flat-roof capacity across orientations; here, the actual module layout is counted separately for each rotated footprint, since packing is one of the study's own variables rather than a fixed input. Electricity generation was estimated using PVGIS rather than the PVsyst software used by Aste et al., with consistent PV technology and loss assumptions applied across the assessed configurations.

2.6 Boundaries adopted and not adopted

Table 2.2 Scope retained from the reference methodology.

Reference element	**Application**
Roof configuration and orientation comparison	Adopted; three orientations and three roof alternatives produce the nine cases.
PV inclination and roof configuration	Comparison of 15° and 35° rack layouts with modules following redesigned roof slopes: 15° for E–W and SE–NW, and 4.93° for N–S. Both specific yield and total roof generation are compared.
Generic solar-suitable area factors	Used as conceptual context only, never multiplied into layouts that are already packed and counted.
Dynamic thermal modelling	Hourly thermal calculation for the proposed envelope, appliance and building-services retrofit.
Variable COP/EER with a 0.91 delivery efficiency	Hourly heating, cooling and hot-water thermal demands are converted into electricity using temperature-dependent COP/EER and an assumed overall distribution, control and emission efficiency of 0.91 (Section 5.3; Appendix B).
Household appliances	Efficient appliances and electric cooking included using household counts, usage assumptions and product consumption data.
Calibration, lifecycle optimisation and cost evaluation	Not claimed for this archetype; these belong to the reference study, not to the work completed here.

The historical comparison uses the national electricity benchmark for households without electric space heating. District heating and central hot-water supply are adopted for the reference-building scenario; their thermal energy is accounted for separately. The proposed retrofit includes heat-pump electricity for these services, alongside cooling, efficient appliances and lighting. The difference between the electricity totals therefore reflects their supply arrangements and demand assumptions, rather than total energy savings.

Sources serve distinct purposes. Historical drawings explain the building type, geometric layouts establish module counts, PVGIS exports quantify generation, and EnergyPlus outputs supply thermal demand and equipment electricity. The district inventory adds measured footprint dimensions and orientations. These records support their respective calculations without substituting for a building survey or measured energy calibration.

2.7 Geometric layout and row spacing

The layouts use LONGi Hi-MO X10 LR7-54HVH-505M modules measuring 1.800 × 1.134 m (LONGi, n.d.), a 20 mm gap between adjacent modules within a row, a 0.50 m usable roof-edge setback, and clear zones around access and ventilation features. On the continuous redesigned surfaces, 20 mm gaps in both directions give repeating dimensions of 1.820 × 1.154 m. For tilted racks, the spacing between rows is calculated separately from their shadow geometry.

The 20 mm packing gap is unrelated to the tilted-row shadow gap, which follows from simple geometry. For a module of slope length L, tilt β and solar altitude α, measured in a section aligned with the shadow, the module's horizontal projection is $L\cos\beta$, its vertical rise is $L\sin\beta$, and the resulting clear shadow gap is approximately:

$$d_{shadow} \approx \frac{L\sin\beta}{\tan\alpha}$$

Rack-row spacing uses a solar altitude of 16.1°, representing solar noon at the winter solstice in Kyiv. The module dimension along the slope is 1.134 m. The clear gap is calculated from the module's vertical rise divided by the tangent of this solar altitude; adding the horizontal module projection gives the row pitch. Clear gaps are approximately 1.0 m for the 15° racks and 2.3 m for the 35° racks, with corresponding pitches of 2.1 m and 3.2 m. This criterion avoids inter-row shading at the selected winter-solstice noon condition. The saved Grasshopper definition retains the unrounded calculation.

2.8 Calculation and reporting rules

Installed DC capacity follows directly from the counted module number:

$$P_{DC} = N \times 0.505\ \text{kWp}$$

where N is the number of whole modules fitted to each case. The module-derived capacity and the entered PVGIS capacity are retained at their original precision in the calculations. Specific yield uses the capacity entered into PVGIS, including its rounding, while installed capacity follows the module count.

$$Y = \frac{E_{PV,\,annual}}{P_{PVGIS}} \quad \left[\frac{\text{kWh}}{\text{kWp} \cdot \text{year}}\right]$$

$$E_{PV,\,MWh} = \frac{E_{PV,\,kWh}}{1000}$$

Annual generation is compared against demand as a simple energy ratio:

$$R_{annual} = \frac{E_{PV,\,annual}}{E_{electricity,\,annual}}$$

The annual generation-to-demand ratio compares two annual energy totals. A value above 100% does not establish hourly self-sufficiency: surplus production can occur at times when demand is low, while imports may still be needed during other hours. Self-consumption requires matching generation and demand at the same time resolution.

All 108 monthly generation values have been checked against the nine PVGIS source tables. Their sums differ from the exported annual totals by less than 0.2 kWh because of source rounding. Annual values therefore use the exported totals. Displayed results are rounded to one decimal place and module counts remain whole numbers; calculations, equation coefficients and technical input specifications retain the precision needed for reproducibility.

2.9 Calculation workflow from geometry to results

The calculations link geometric layout, solar exposure, electrical generation and demand through the following tools.

1. Rhino represents the five-storey building and its three long-axis orientations. For each orientation, Grasshopper defines south-facing racks at 15° and 35° and a continuous redesigned roof, giving nine configurations.
2. Grasshopper, working parametrically on Rhino geometry, places and counts whole PV modules on each roof variant under the constraints set out in Sections 2.2, 2.3 and 2.7 (module size, packing gap, edge setback, and retained access/ventilation clearances). This is the step that produces the module count N for each of the nine cases which is a counted result, not an area-based estimate.

3. Ladybug uses the roof geometry and weather data to calculate annual incident radiation and radiation roses. These explain exposure and local shading; PVGIS supplies the electricity-generation values.
4. PVGIS evaluates each roof using its installed capacity, tilt and azimuth at 50.455° N, 30.519° E. The resulting annual and monthly generation values are used in the building-scale comparisons.
5. Honeybee and OpenStudio translate the building geometry, envelope, occupancy and use assumptions into an EnergyPlus simulation. Electricity use for efficient appliances and cooking is estimated from household and resident counts, published usage assumptions and product specifications. This estimate is translated into an apartment equipment power density and applied through the equipment schedule. The annual simulation is rerun to account for the resulting internal heat gains. The exported hourly heating, cooling and hot-water thermal demands are then converted separately into electricity using temperature-dependent COP/EER and the assumed overall system efficiency of 0.91. Appliance and lighting electricity is taken directly from EnergyPlus and requires no heat-pump conversion (Section 5.3)
6. QGIS measures the dimensions and orientations of 63 residential roof units in Vidradnyi's microdistrict. Whole-module layouts are generated for adapted longitudinal and transverse slopes; PVGIS supplies the corresponding yields and the higher annual generation is selected for each unit. The maps retain the link between roof geometry, installed capacity and output.

All nine PVGIS calculations use the PVGIS-SARAH3 radiation database, crystalline-silicon technology, a calculated terrain horizon and a 14% user-entered system-loss allowance. The modules follow the redesigned roof slopes and are proposed on supports that maintain a ventilated gap above the roof covering. The PVGIS free-standing setting was adopted to represent the assumed free airflow behind the modules (European Commission Joint Research Centre, n.d.-a).For the N–S redesigned roof, the inclination entered into PVGIS was 4.93°; the exported report displays 5°.

The final retrofit calculation uses EnergyPlus 25.1.0 and the Kyiv station 333450 TMYx 2011–2025 weather file. The SQL, IDF and completion logs are retained together. The 8,760 hourly outputs are aggregated independently, and their temperature-dependent electricity conversion is checked against monthly and annual totals. The final PixelCounting run completes successfully with zero severe errors.

3 Kyiv and the representative building

3.1 Energy resilience and the case for Kyiv

Kyiv's renovation needs are shaped by global climate objectives and the damage to Ukraine's energy infrastructure since Russia's full-scale invasion in February 2022. Attacks on power stations, district-heating plants and distribution networks have repeatedly disrupted electricity, heating and hot-water supplies, affecting homes and public services. Many residential buildings depend on centralised systems for space heating and domestic hot water. These disruptions reinforce the need for more resilient energy provision, with distributed electricity generation contributing alongside building renovation and improvements to heating infrastructure.

The IEA's 2024 analysis of Ukraine's energy security describes the vulnerability of large, centralised generating units and the resulting shift toward decentralised resources — including rooftop solar paired with storage for public buildings, households and businesses (IEA, 2024a). Its companion report on building a decentralised electricity system places rooftop PV within a broader mix of generation, storage and network measures (IEA, 2024b). Both are dated analyses of a system that keeps changing; they establish the reconstruction rationale for distributed generation without standing in for current capacity or damage totals.

Existing roofs offer space for generation distributed across a residential district. Supporting essential loads during an outage would additionally require appropriate electrical arrangements, storage and controls. The generation estimates establish the scale of the roof resource, while backup operation remains a separate design task.

Kyiv is a relevant setting precisely because many of its residential districts contain repeated Soviet-era apartment-block forms whose roofs can be studied as a family of potential interventions. That repetition is what makes a representative-building method useful in the first place; the variation in orientation and actual physical condition is exactly what makes unrestricted replication inappropriate. The study treats this standardisation as a reason to investigate transferability — not as evidence that one system will fit every block.

The characteristic roofscape offers opportunities for PV installation, while roof obstructions, maintenance access and edge clearances limit the space available. The nine configurations incorporate the adopted obstructions and access requirements of the reference building. Comparing layouts within these constraints shows how building orientation and roof form influence module capacity and annual electricity generation. The roof strategy is then adapted to the different dimensions and orientations of the residential blocks in Vidradnyi.

3.2 Existing solar research and the scale of inference

Winkler and colleagues' national rooftop-PV assessment provides useful context for this approach (Winkler et al., 2025). It combines satellite-derived building data with footprint-to-roof and roof-to-capacity factors developed from high-resolution German data, then models generation across the country. The study explicitly ties its transfer assumption to similarities in building stock and urban form, and reports 238.8 GW and 290 TWh/year of national potential, excluding north-facing surfaces — a modelled national potential, not an installed capacity or a measured generation figure.

The methodological lesson is to keep each step from spatial data to electrical output explicit. A national assessment cannot validate the module count or shadow environment of one roof. Conversely, a detailed building calculation cannot establish a city-wide total. The district assessment therefore documents its own selected roofs, dimensions and layouts.

Whole-module placement explains why roofs with similar nominal areas can accommodate different capacities. National research provides wider context, while the detailed building comparison supplies roof strategies that are adapted to the geometry of Vidradnyi.

3.3 Electricity and heat in the residential context

The residential comparison distinguishes electricity from separately supplied thermal energy. District heating and central hot-water supply are assumed for the reference-building scenario. The national household-electricity statistic identifies households without electric space heating, but does not separately resolve each electrical end use. The electrified retrofit adds heat-pump electricity for heating and hot water, so the comparison describes different supply and demand arrangements rather than measured total energy savings.

The existing-energy reference adopted in this project is a Ukrainian household-electricity statistic for 2020, reported as 168 kWh per household per month for households without electric heating (State Statistics Service of Ukraine, n.d.). It is a historical benchmark, not a live Kyiv utility bill or a complete hourly load profile, and Chapter 5 records how it is applied to the 30-apartment archetype and where the separate common-lighting assumption enters the calculation.

Power-to-heat remains a plausible connection between local electricity generation and the city's existing heat networks: surplus electricity could run heat pumps, and a properly designed thermal store could shift heat delivery in time. But whether that connection is actually useful depends on the receiving network's temperatures, heat demand, storage capacity and operating rules — the pipes and water already in the network cannot simply be assumed to offer unlimited, loss-free seasonal storage. The

district generation total does not establish an available heat-network surplus; that would require simultaneous electricity and heat demands.

3.4 Kyiv solar conditions in the adopted runs

The location is fixed across all nine simulations at 50.455°N, 30.519°E. Exported annual in-plane irradiation comes out at 1,396.5 kWh/m² for south-facing 35° surfaces, 1,322.8 kWh/m² for south-facing 15° surfaces, 1,280.1 kWh/m² for the southeast-facing 15° redesigned roof, and 1,243.4 kWh/m² for the shallow N–S redesigned roof, as represented in PVGIS (European Commission Joint Research Centre, n.d.-a). These values represent the annual solar energy received per square metre of each inclined PV surface, accounting for its tilt and orientation.

June generation substantially exceeds December generation in all nine cases. This seasonal concentration matters when PV is compared with heat-pump electricity, since the largest heating requirement occurs when solar production is low.

3.5 Historical construction and archetype provenance

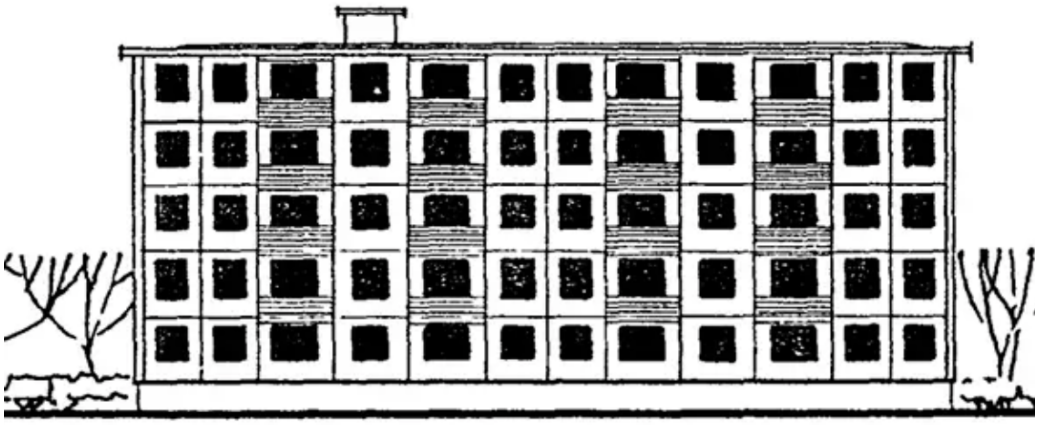

Figure 3.1 Elevation of the five-storey, 30-apartment building, standard project 1-480A-31. Source: KievZNIIEP (n.d.), passport, sheet 1; project introduced in 1964.

The representative building has five storeys, two sections, 30 apartments and 80 nominal residents. Its historical reference is standard project 1-480A-31, developed by KievZNIIEP, approved in 1963 and introduced in 1964. The passport shows the elevation and typical floor plan of a repeated large-panel housing type. The energy assessment uses a simplified geometric reconstruction rather than a survey of a particular Kyiv address.

The historical drawings show a repetitive apartment/stair organisation and a large-panel construction vocabulary. They explain why a compact rectangular roof and recurring service and access features are appropriate subjects for architectural abstraction — but they do not establish the remaining load capacity of a present-day building. Adding a roof intervention on a real building would require its own structural checks of panels, joints, load paths, foundations, and wind and snow actions.

The conditioned reference area is 1,697.0 m², obtained from the 30 apartment-zone floor polygons. A further 140.4 m² represents unconditioned stair and circulation spaces. Together they occupy 1,837.4 m² across five storeys, based on the 34.8 × 10.56 m reference footprint. Energy intensities use the conditioned zone area consistently; household counts and occupancy define the appliance allowance.

3.6 From historical plan to representative geometry

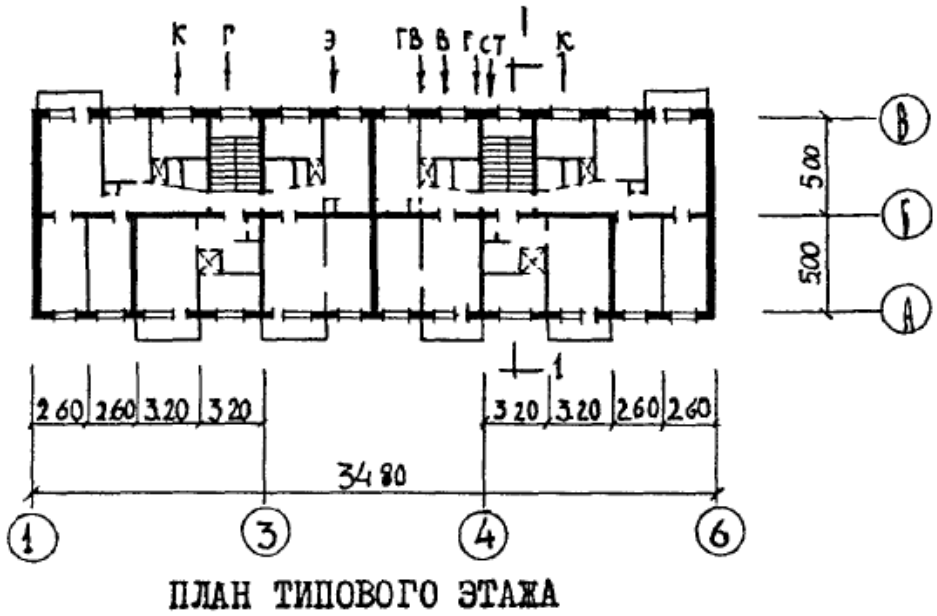

Figure 3.2 Typical floor plan of standard project 1-480A-31, showing the two-section arrangement and 34.8 m length. Source: KievZNIIEP (n.d.), passport, sheet 1; project introduced in 1964.

The passport's typical floor plan establishes the repeated two-section arrangement. Geometric reconstruction makes the roof configurations comparable, while an eventual intervention would need a building survey to establish actual dimensions and condition. The final layouts and module counts define the energy comparison.

The working geometry, roof layouts and module counts are retained with the calculation records. The 1-480A-31 passport documents the historical building type, with its elevation, typical plan and construction information (KievZNIIEP, n.d., sheets 1–2).

3.7 Final architectural configurations

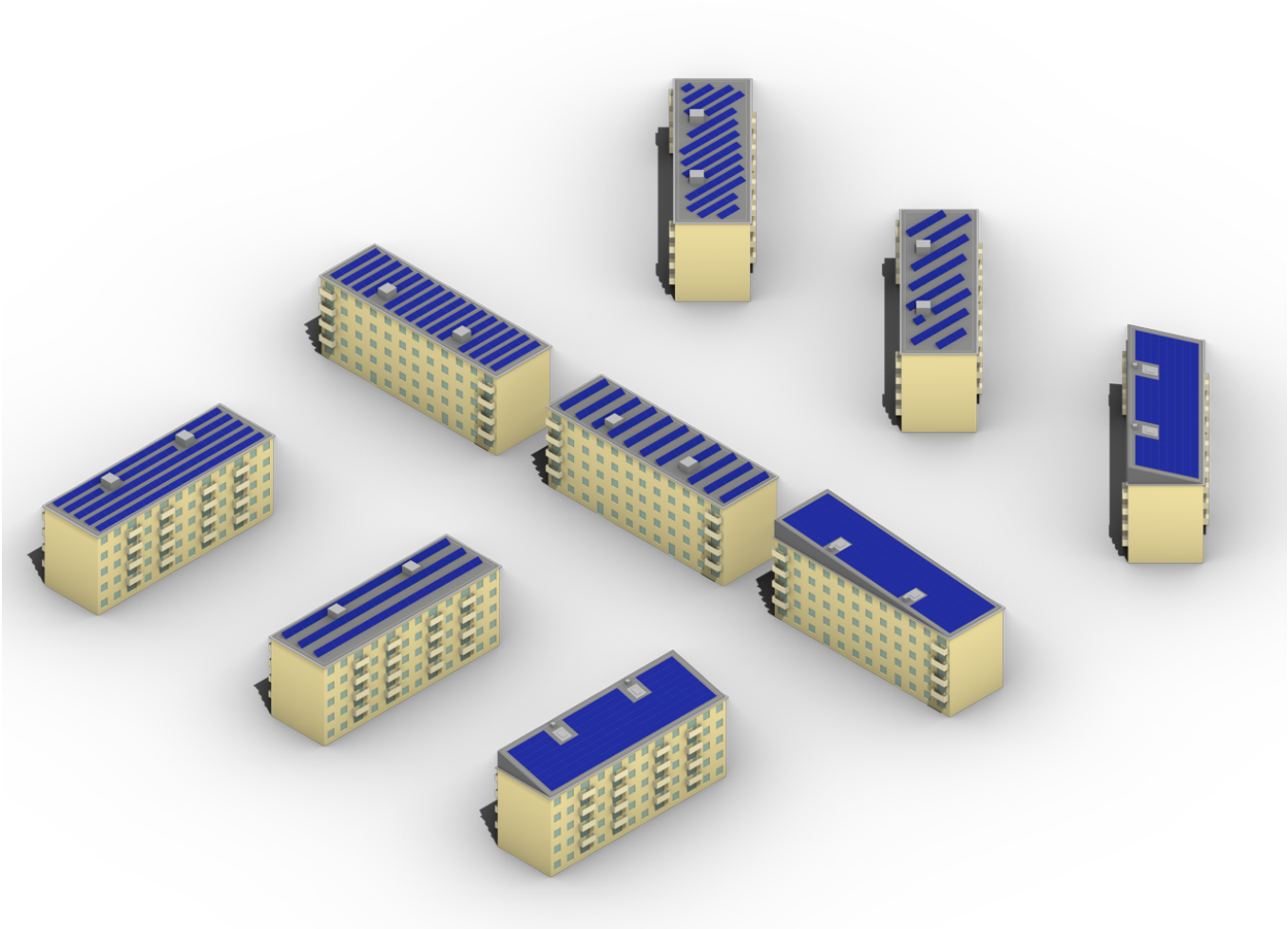

Figure 3.3 Final isometric presentation of the nine roof cases. These are variants of one representative building, not a built district. Source: author.

The rack-mounted cases retain south-facing PV rows at 15° and 35°. The redesigned cases instead use a continuous PV-bearing slope: for the east–west orientation, the adopted surface is south-facing at 15°; for north–south, the extended south-facing surface has a shallow 4.9° inclination; for southeast–northwest, the roof surface is inclined at 15° and faces southeast, corresponding to PVGIS azimuth −45°.

The redesigned roof is not just a different rack tilt — it changes the available continuous surface and reduces the need for spacing between separate raised rows, though roof access and penetrations still constrain where modules can actually sit. In the thermal scenario described in Chapter 5, the sloping over-roof is treated as unheated shading above the insulated flat roof, so it is not automatically part of the conditioned envelope.

4 Photovoltaic results and solar assessment

4.1 The adopted nine-case matrix

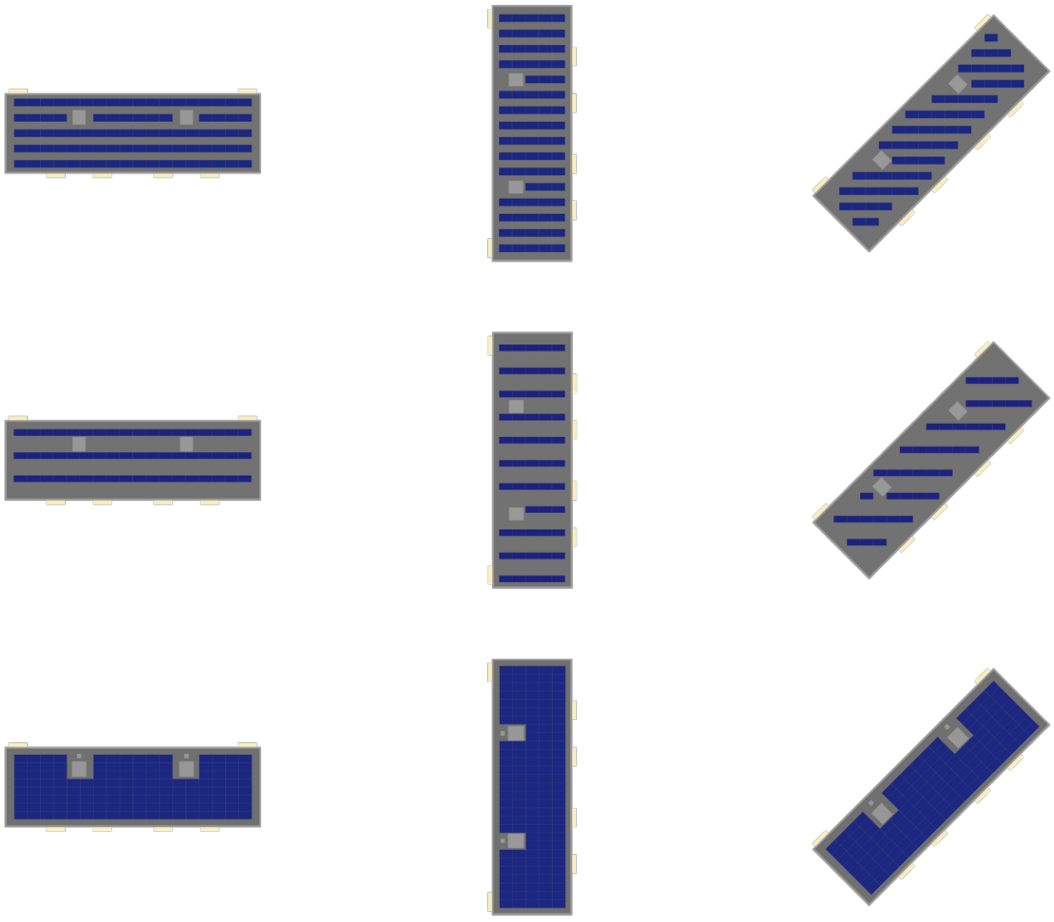

Figure 4.1 Final top-view layouts. Columns: E–W, N–S, SE–NW. Rows: 15° racks, 35° racks, redesigned roofs. Module orientation must be read separately from building-axis orientation. Source: author.

The comparison evaluates both total annual electricity and annual specific yield. The redesigned roofs produce the largest total in every building orientation. South-facing 35° racks produce the most electricity per installed kWp among the tested alternatives, but accommodate fewer modules — establishing a roof-level packing trade-off rather than a single, universally best inclination.

Table 4.1 presents annual generation, capacity and specific yield to one decimal place. The calculations retain the original PVGIS precision.

4.2 Verified annual generation

Table 4.1 Nine-case PV comparison. Installed capacity follows whole-module counts; specific yield uses the entered PVGIS capacity. Source: author's layouts and PVGIS.

Case	N	Capacity kWp	Energy MWh/year	Yield kWh/kWp/year
N–S rack 35°	53	26.8	29.8	1114.0
N–S rack 15°	76	38.4	40.3	1049.3
N–S redesigned	137	69.2	67.8	980.4
E–W rack 35°	54	27.3	30.4	1114.0
E–W rack 15°	86	43.4	45.6	1049.3
E–W redesigned	132	66.7	69.9	1049.3
SE–NW rack 35°	41	20.7	23.1	1114.0
SE–NW rack 15°	58	29.3	30.7	1049.3
SE–NW redesigned	132	66.7	67.6	1013.7

The E–W redesigned roof produces 69.9 MWh/year, followed by N–S at 67.8 and SE–NW at 67.6 MWh/year. The highest-to-lowest difference is 2.4 MWh/year, or 3.5% of the lowest redesigned-roof output. The N–S result exceeds SE–NW by only 0.3 MWh/year — approximately 0.4% — and this small separation should not be treated as a robust construction preference without additional shading and feasibility evidence.

The three redesigned roofs therefore converge in annual production despite different surface orientations and capacities. The N–S case reaches this through 137 modules, while the other two use 132. This is the central architectural result of the comparison: greater accommodated capacity can offset a less productive orientation or tilt per installed kWp.

4.3 Tilt and azimuth input checks

Table 4.2 Tilt and azimuth values entered into PVGIS for each case.

PV surface	Tilt	PVGIS azimuth
All 35° rack cases	35°	0° south
All 15° rack cases	15°	0° south
N–S redesigned	4.93° input; 5° in export	0° south
E–W redesigned	15°	0° south
SE–NW redesigned	15°	–45° southeast

4.4 Installed capacity and roof packing

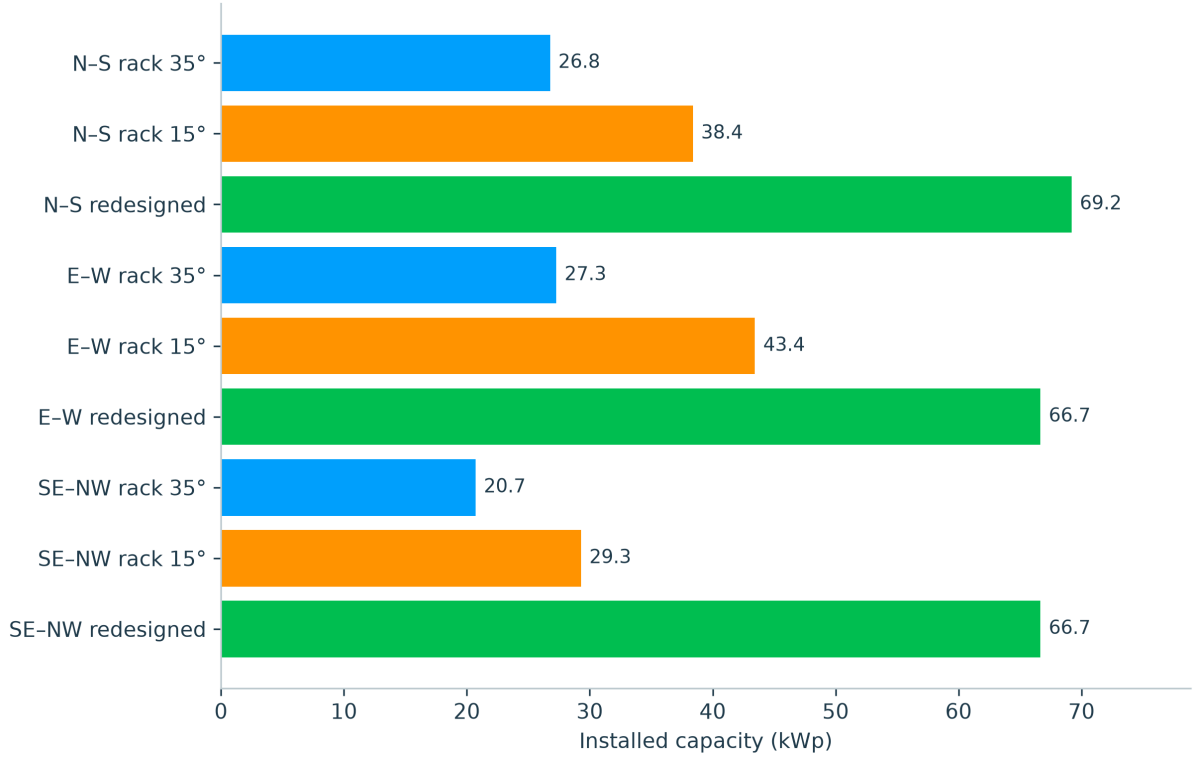

Figure 4.2 Installed capacity from the whole-module layouts. Source: author's module counts, using 505 W per module.

The redesigned layouts accommodate 132–137 modules, corresponding to 66.7–69.2 kWp. The 35° rack layouts contain 41–54 modules; the 15° rack layouts contain 58–86. Relative to the same-axis 15° racks, module-derived capacity increases by 80.3% for N–S, 53.5% for E–W and 127.6% for SE–NW.

The capacity gain follows from geometry and module arrangement. A continuous roof plane accommodates an extensive, regular array while retaining access and ventilation clearances. The layouts were optimised for the reference roof dimensions and the adopted design constraints.

For the QGIS transfer in Chapter 6, these counts are representative-case outputs, not constants that can be assigned to every five-storey building. A longer roof, a different aspect ratio or a changed service enclosure can alter both the packing achieved and the height needed to maintain the same roof slope.

4.5 Annual electricity generation

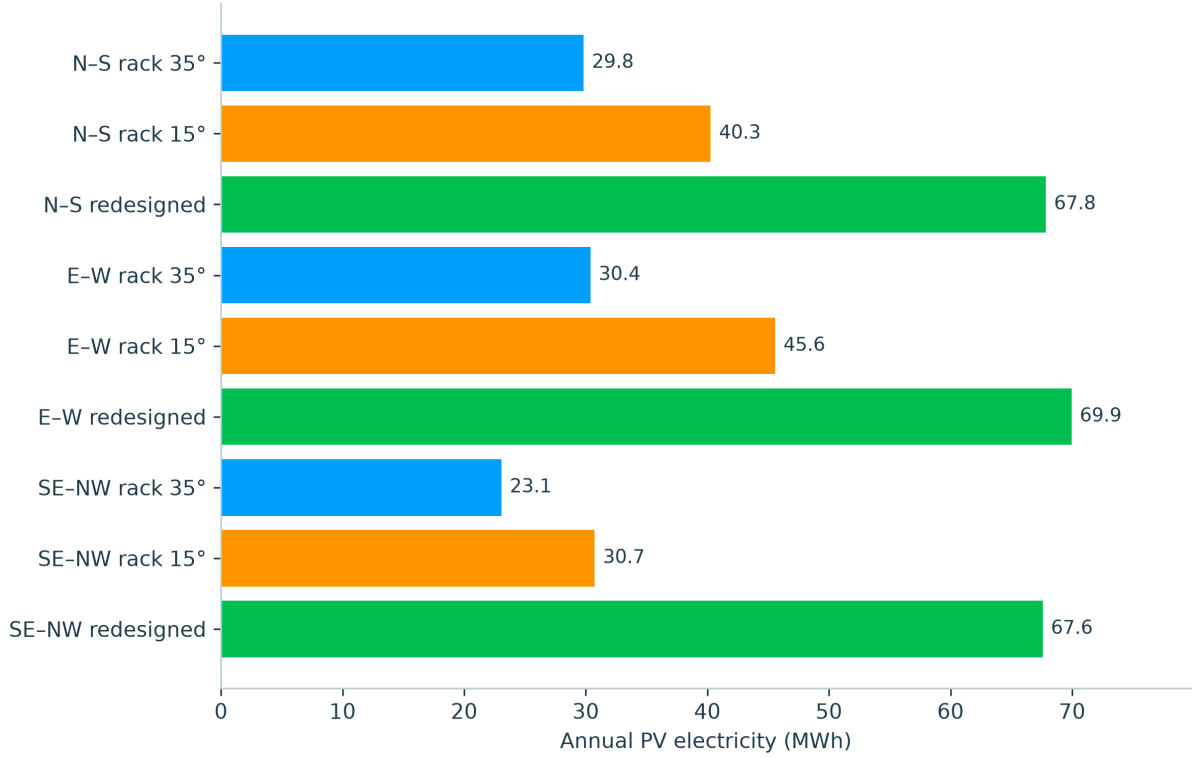

Figure 4.3 Annual modelled PV generation of the nine layouts, checked against the source exports. Source: author, from PVGIS.

Compared with the corresponding 15° rack layouts, annual generation increases by 68.4% for N–S, 53.5% for E–W and 119.9% for SE–NW. All three redesigned roofs therefore exceed the existing-roof alternatives in annual building-level generation.

The E–W comparison is the most direct of the three, since both alternatives face south at 15° and therefore share effectively the same specific yield: the increase from 43.4 to 66.7 kWp produces a correspondingly proportional increase in production. In the N–S and SE–NW comparisons, by contrast, a larger array outweighs a lower specific yield, so capacity and orientation effects act in opposite directions.

This ranking reflects modelled, long-term average production under common PVGIS assumptions. The roof with the highest annual generation is not necessarily the cheapest, the most structurally feasible, the easiest to maintain, or the best matched to actual demand — those remain separate design criteria, addressed only partially in Chapter 5.

4.6 Specific yield and the tilt trade-off

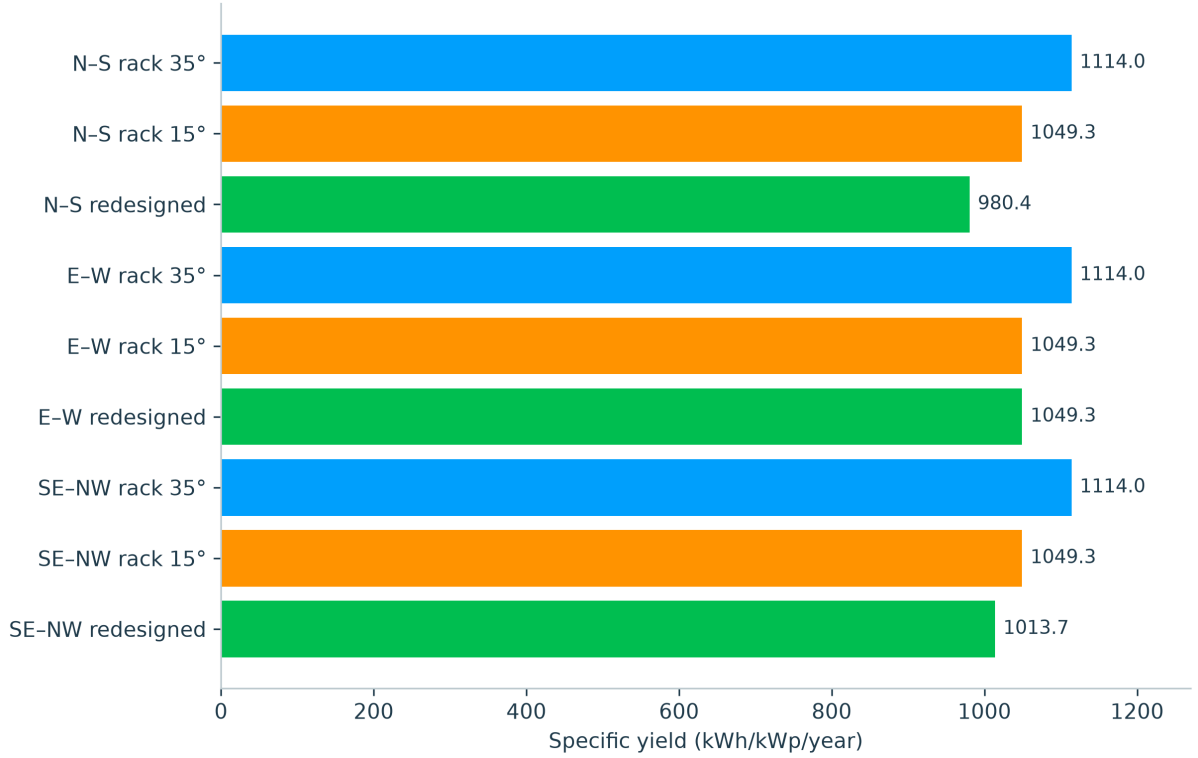

Figure 4.4 Annual specific yield using each case's PVGIS entered capacity. Source: author, from PVGIS exports.

The 35° south-facing configurations yield approximately 1,114.0 kWh/kWp/year. South-facing 15° configurations yield 1,049.3; the southeast-facing 15° roof yields 1,013.7; and the shallow N–S redesigned roof yields 980.4. The highest production per unit of installed power therefore occurs in the cases with the lowest total installed roof capacity.

The E–W and SE–NW redesigned roofs share the same module count, capacity and tilt; their production differs by 3.4% relative to E–W, which is consistent with the azimuth change alone under the shared simulation assumptions. The N–S case has the lowest specific yield yet the greatest installed capacity — comparing cases by kWh/kWp alone would miss its competitive roof-level energy total.

South-facing 35° racks achieve the highest specific yield among the selected configurations. Their lower module count, however, limits total roof generation. The continuous redesigned surfaces use the available roof area more extensively, which is the principal advantage demonstrated by the comparison.

4.7 Monthly generation for the north–south building

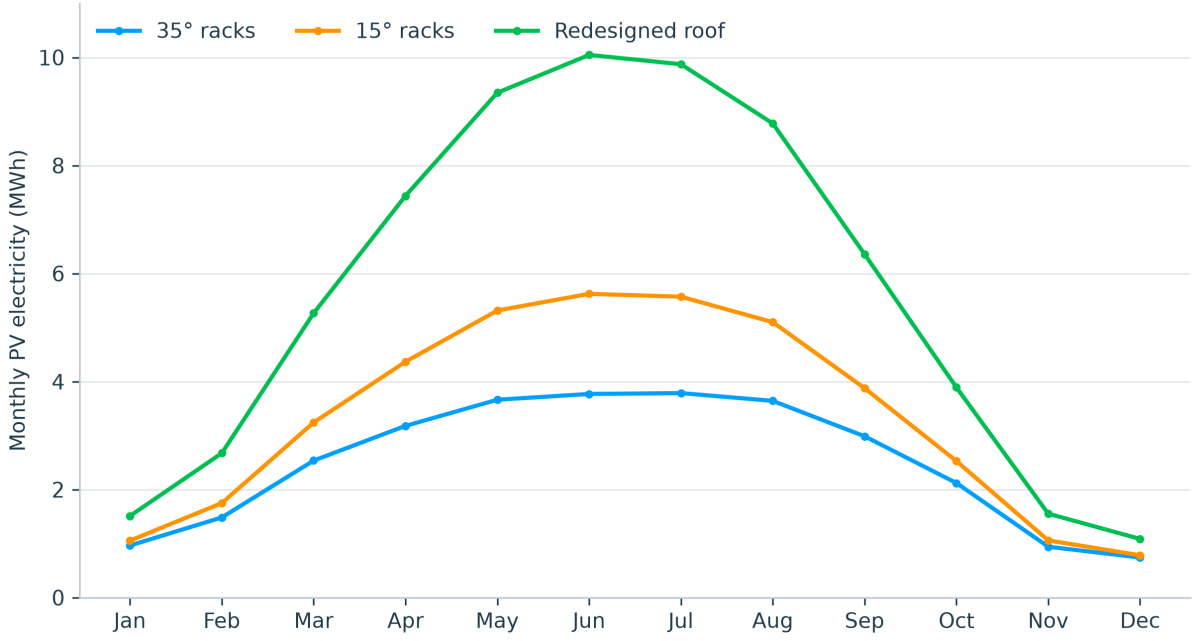

Figure 4.5 N–S average monthly PV generation in MWh; native monthly source values appear in Appendix A. Source: author, from PVGIS exports.

The N–S redesigned roof exceeds both rack layouts in all twelve months, reaching 10.0 MWh in June and falling to 1.1 MWh in December. April–September contributes approximately 76.4% of the annual total. Its large array improves winter production in absolute terms, but the shallow plane still produces a particularly strong summer concentration.

These are average monthly PVGIS values, not observations from any single operating year. A monthly total describes seasonal balance, but it cannot identify midday export, night-time import or actual self-consumption — the later demand comparison in Chapter 5 has to preserve the same time resolution and identify the source of each monthly demand component in turn.

4.8 Monthly generation for the east–west building

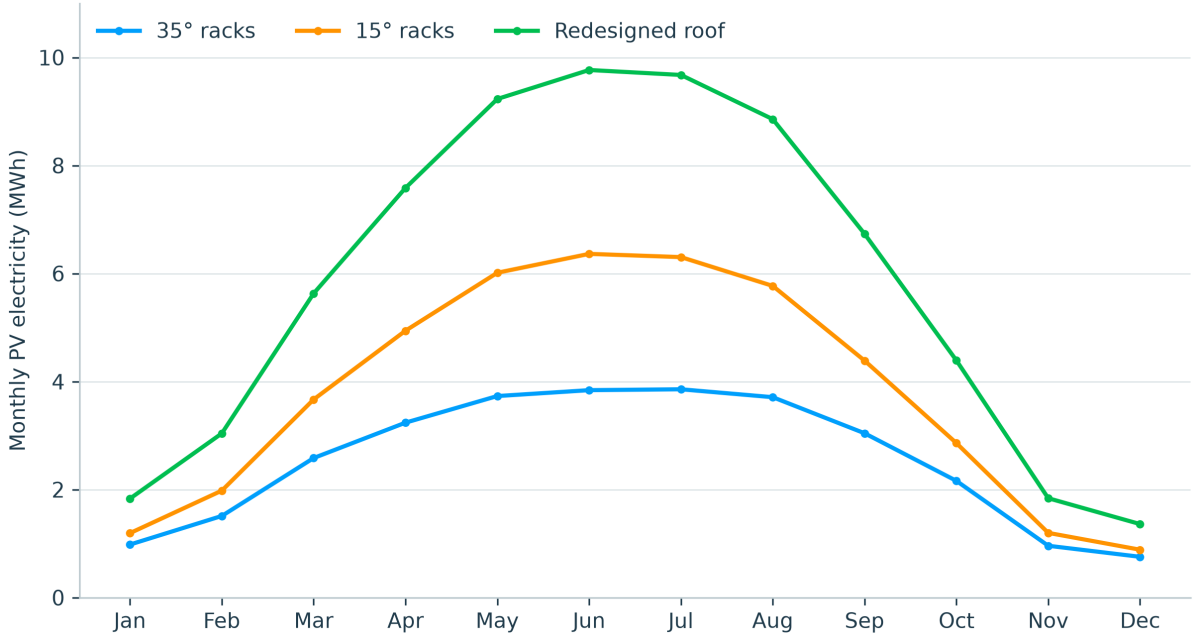

Figure 4.6 E–W average monthly PV generation in MWh; native monthly source values appear in Appendix A. Source: author, from PVGIS exports.

The E–W redesigned roof produces 9.8 MWh in June and 1.4 MWh in December. Its monthly profile has essentially the same shape as the E–W 15° rack case, since tilt and azimuth are identical between them; production is around 1.5 times larger simply because capacity increases. April–September contributes approximately 74.1% of annual generation.

4.9 Monthly generation for the southeast–northwest building

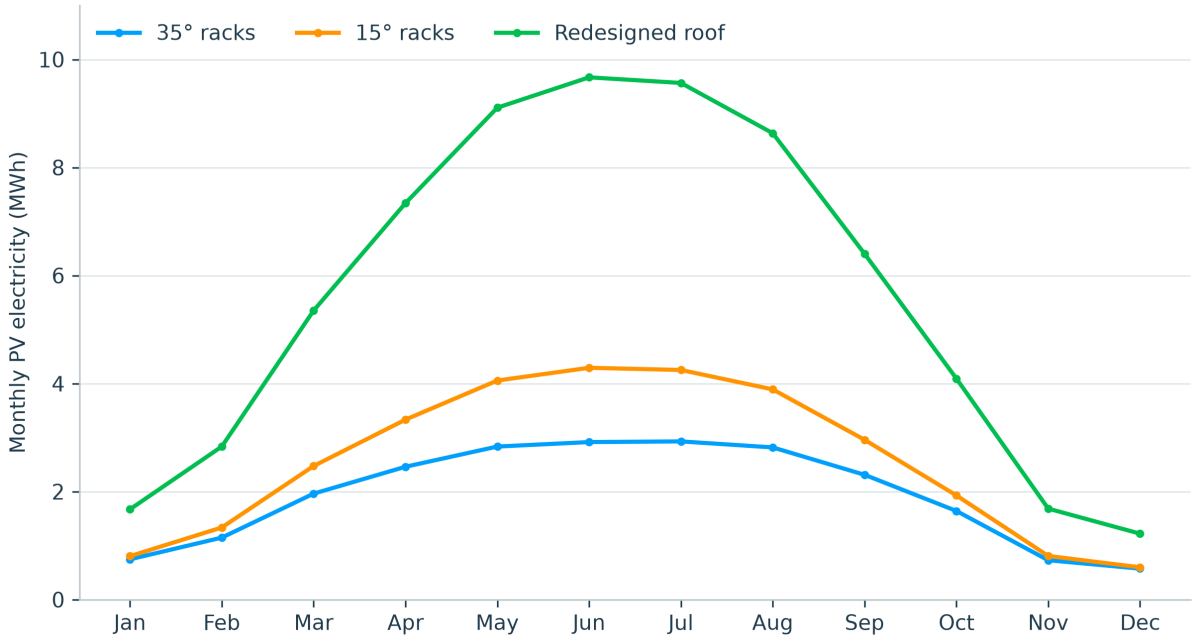

Figure 4.7 SE–NW average monthly PV generation in MWh; native monthly source values appear in Appendix A. Source: author, from PVGIS exports.

The southeast-facing redesigned roof exceeds both south-facing rack cases in every month. June production is 9.7 MWh, compared with 1.2 MWh in December, with approximately 75.1% of annual generation occurring in April–September. The capacity gain dominates the reduction in specific yield caused by the changed orientation and tilt relative to the 35° reference case.

4.10 Monthly comparison of the redesigned roofs



Figure 4.8 Monthly generation of the three redesigned roofs, plotted on consistent scales across the twelve panels. Source: author, from PVGIS exports.

E–W leads in nine months of the year, while N–S leads in May, June and July, by 116.0, 278.8 and 198.9 kWh respectively. E–W nevertheless retains the highest annual output overall, and the southeast-facing roof produces less than E–W in every single month.

The Vidradnyi calculations therefore use each adapted roof's actual tilt and direction in PVGIS. This preserves orientation-specific annual and monthly generation without assigning every roof the east–west profile.

4.11 Incident-radiation assessment

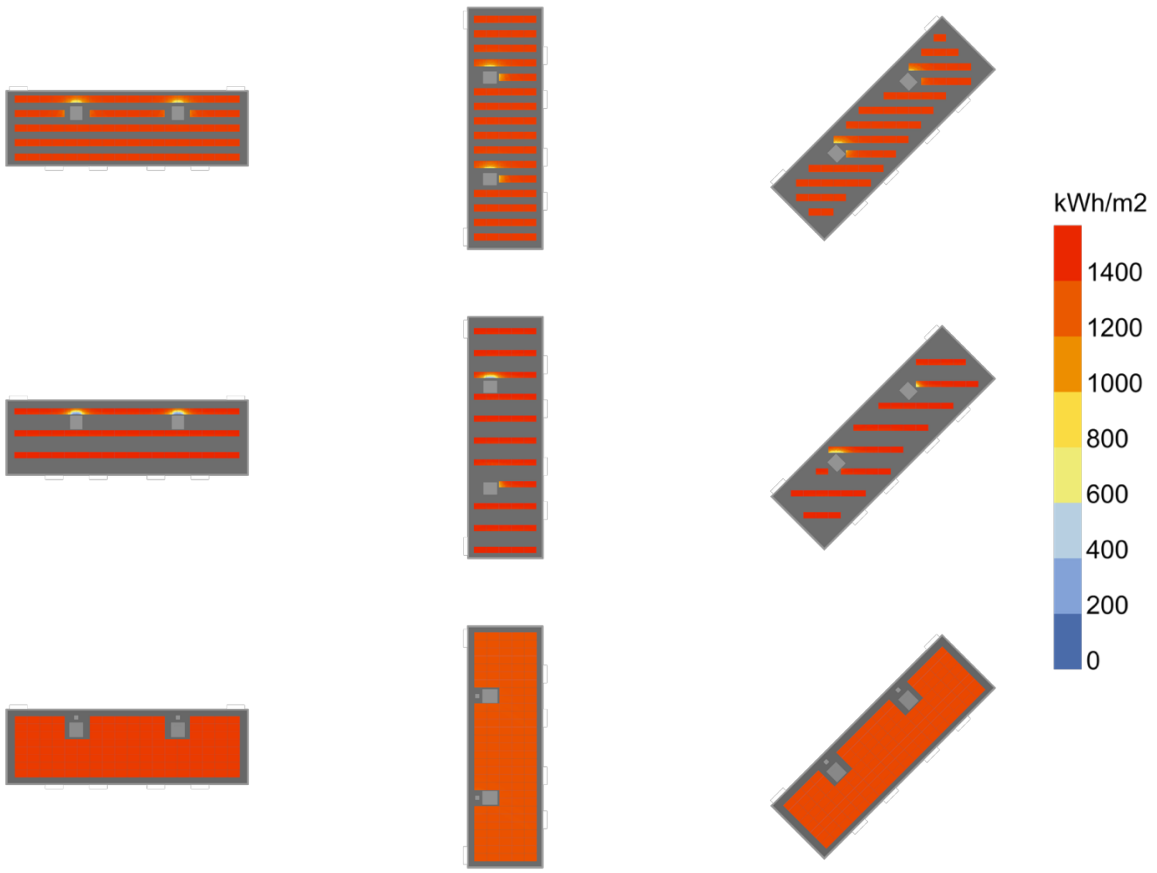

Figure 4.9 Ladybug annual incident-radiation comparison. Columns: E–W, N–S, SE–NW; rows: 15° racks, 35° racks, redesigned roofs. Values are annual incident radiation in kWh/m². Source: author.

The diagrams show how solar exposure varies across the nine roof configurations. Most panel surfaces receive relatively uniform radiation, while lower exposure around roof enclosures indicates local shading. These patterns help identify shaded areas that are not represented in the annual PVGIS electricity totals.

Annual incident solar radiation was calculated in Ladybug 1.10.0 using the Kyiv SRC-TMYx weather file for 2011–2025. All nine roof configurations were assessed over the full year on a 0.10 m grid, with north aligned to Rhino's positive Y-axis. The PV geometry and rooftop obstructions were included in the analysis. A shared legend ranging from 0 to 1,400 kWh/m² allows direct visual comparison of radiation across the arrays and highlights local variations around rooftop obstructions.

Ladybug is used to assess how roof geometry and obstructions affect solar exposure. Annual electricity generation is estimated separately with PVGIS, without an

additional adjustment for local shading from roof obstructions or neighbouring module rows.

4.12 Radiation rose at 4.9°

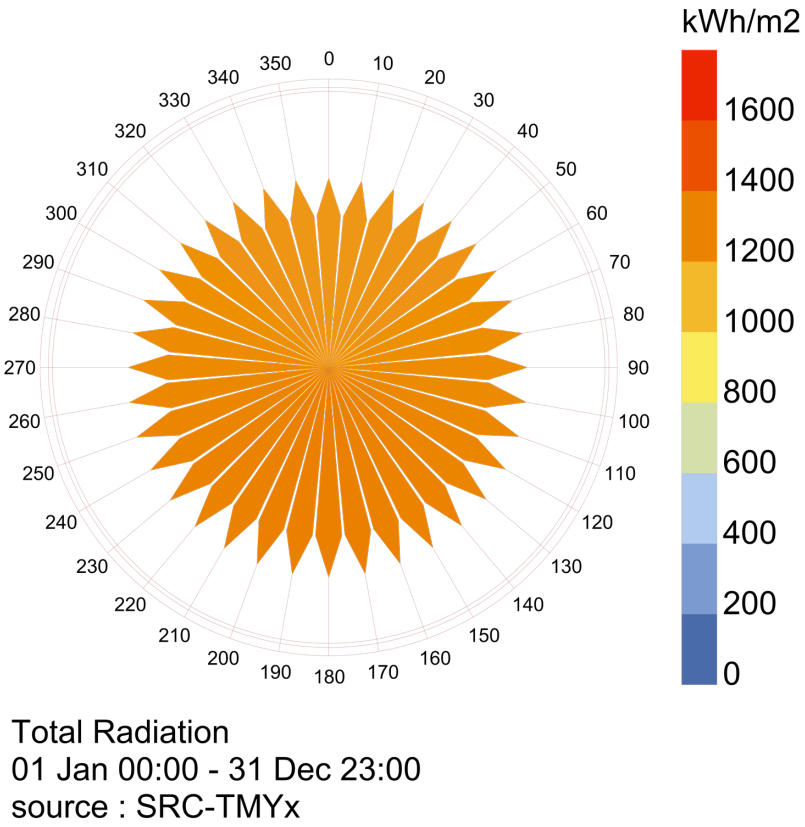

Figure 4.10 Completed annual radiation rose at 4.9°, reporting total radiation from 1 January to 31 December using the SRC-TMYx source weather file. Source: author.

The shallow 4.9° surface shows the most uniform directional pattern of the three roses. Its relatively limited azimuth contrast should be read alongside the lower specific PV yield of the adopted N–S roof: more modules, rather than a superior per-kWp resource, explains its competitive annual generation.

4.13 Radiation rose at 15°

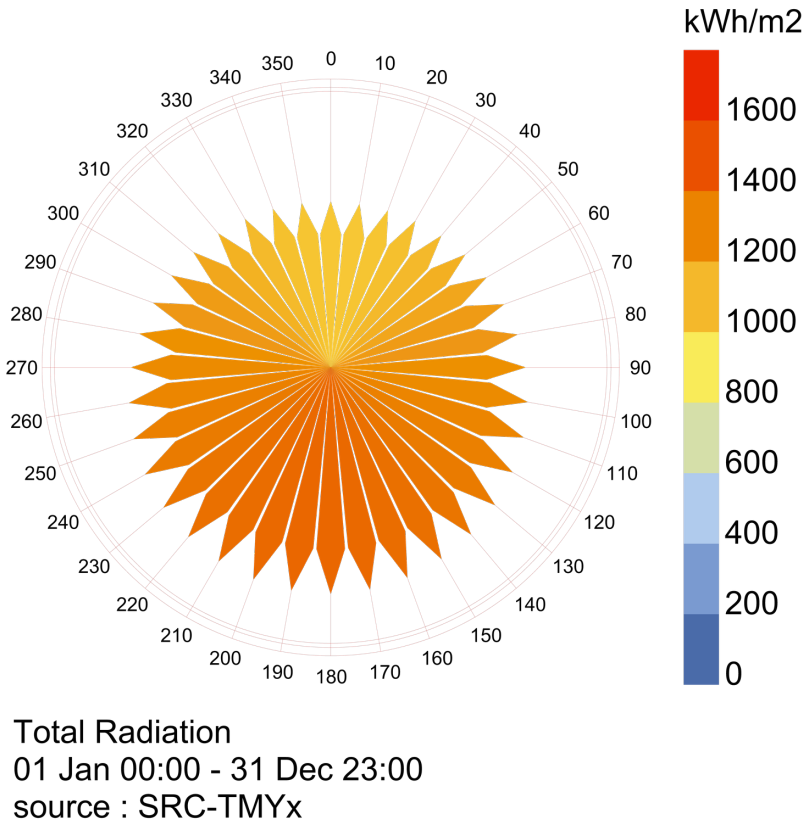

Figure 4.11 Completed annual radiation rose at 15°, reporting total radiation from 1 January to 31 December using the SRC-TMYx source weather file. Source: author.

At 15°, a clear directional difference is visible. The project retains a south-facing E–W roof and a southeast-facing SE–NW roof at this same inclination, so their generation comparison isolates the azimuth effect under equal installed power and shared PVGIS assumptions.

4.14 Radiation rose at 35°

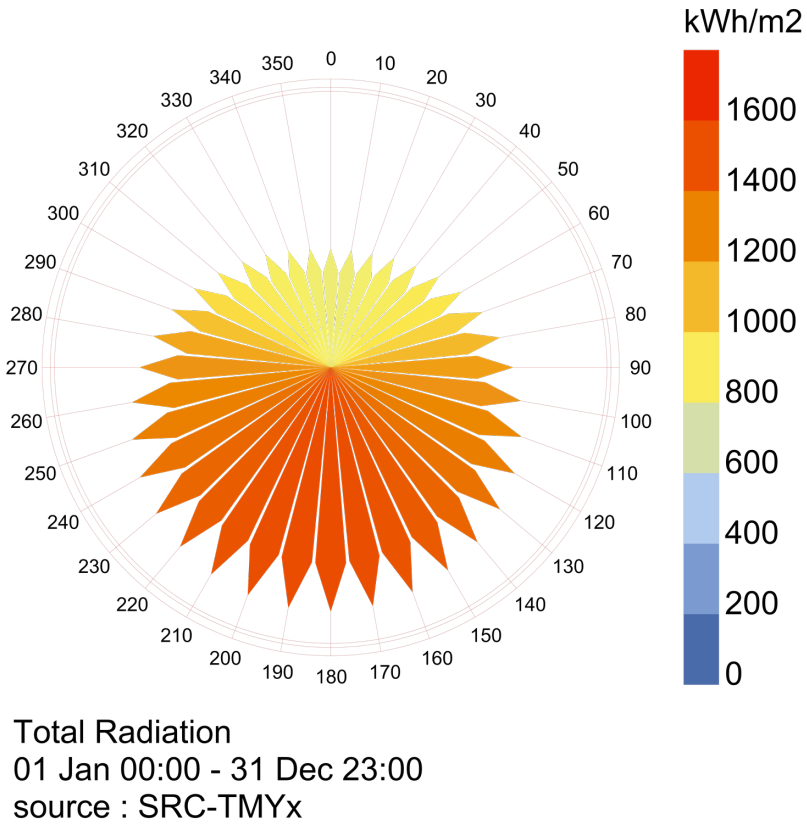

Figure 4.12 Completed annual radiation rose at 35°, reporting total radiation from 1 January to 31 December using the SRC-TMYx source weather file. Source: author.

At 35°, the directional contrast is strongest. South-facing rack cases achieve the highest specific yield in the tested set, but their row spacing and roof-boundary fit limit total capacity. The rose supports an exposure interpretation, not a conclusion about how many modules fit: its petals represent solar exposure by direction, not building module counts or electricity production.

The shallow-angle rose is visually more uniform around the azimuth circle, while directional contrast becomes more pronounced at larger tilt — consistent with the interpretation that the shallow N–S roof is less azimuth-sensitive, but receives a different annual and seasonal resource overall.

4.15 Roof design and photovoltaic performance

The comparison shows the benefit of redesigning the roof to accommodate a larger photovoltaic array. The continuous roof configurations produce more annual electricity than the tested rack layouts, primarily because they accommodate more

installed capacity. The E–W redesigned roof achieves the highest calculated annual generation, while the N–S and SE–NW alternatives produce similar totals. The larger difference between redesigned roofs and rack layouts highlights the importance of usable roof area, module arrangement and architectural integration.

The results also reveal a distinction between specific yield and total generation. The 35° rack configurations achieve higher output per installed kilowatt, but their spacing requirements limit the number of modules. The redesigned roofs achieve greater total production by combining suitable solar exposure with more extensive use of the available surface.

PVGIS provides the annual and monthly electricity estimates, including its system-loss and environmental-loss calculations. These values represent expected generation under the adopted weather conditions; individual years will vary. The Ladybug maps complement the comparison by showing local radiation and shading patterns, without applying a separate electrical shading correction.

Together, the findings support roof renovation as a means of increasing photovoltaic capacity on the reference building and across Vidradnyi. Detailed structural assessment and construction design form the next stage in developing these proposals for implementation.

5 Electricity demand and the electrified retrofit

5.1 Historical household electricity reference

The reference household electricity demand is 168 kWh per month, reported for Ukrainian households without electric heating in 2020 (State Statistics Service of Ukraine, n.d.). For 30 apartments, 168 × 12 × 30 gives 60,480.0 kWh/year, including appliances and apartment lighting. An estimated communal-lighting allowance of 2,885.0 kWh/year, adopted from the retrofit assessment, brings the reference to 63,365.0 kWh/year, or 63.4 MWh/year.

Rooftop PV generation is compared with two annual electricity demands: the historical household and communal benchmark, and the fully electrified retrofit. In the historical scenario, heating and hot water are supplied separately by district systems. In the retrofit, their heat-pump electricity is included alongside appliances, lighting and cooling. The comparison shows how much of each scenario's annual electricity demand rooftop PV could generate; assessing total energy savings would also require the historical consumption of district heating and hot water

.Table 5.1 Annual PV generation relative to the historical household-electricity benchmark.

PV option	Annual PV MWh	PV / 63.4 MWh reference
N–S rack 35°	29.8	47.1%
N–S rack 15°	40.3	63.6%
N–S redesigned	67.8	107.0%
E–W rack 35°	30.4	47.9%
E–W rack 15°	45.6	71.9%
E–W redesigned	69.9	110.4%
SE–NW rack 35°	23.1	36.4%
SE–NW rack 15°	30.7	48.5%
SE–NW redesigned	67.6	106.6%

All three redesigned roofs generate slightly more electricity over the year than the 63.4 MWh historical benchmark. Their annual production ranges from 67.6 to 69.9 MWh, equivalent to 106.6–110.4% of household and communal electricity demand. The rack layouts provide lower annual coverage, ranging from 36.4% to 71.9%. For each orientation, the 15° rack layout produces more electricity than the 35° alternative

because its greater installed capacity outweighs its lower yield per installed kilowatt-peak. The redesigned roofs therefore match or exceed the historical demand on an annual basis, although grid exchanges still depend on when electricity is generated and used.

5.2 Envelope, comfort and efficient appliances

The retrofit retains 30 apartments and 80 residents, with a conditioned reference area of 1,697.0 m² and 140.4 m² of unconditioned circulation. It combines insulation, improved glazing, seasonal solar control, efficient household appliances and heat-pump supply. The sloping PV roof shades the insulated flat roof and remains outside the conditioned enclosure.

Table 5.2 Adopted retrofit assumptions.

Component	Adopted treatment
Opaque envelope	Wall: 120 mm stone wool + 350 mm representative lightweight concrete. Flat roof: 250 mm stone wool + 100 mm equivalent concrete.
Floor and zoning	Ground-contact floor: 180 mm XPS + 100 mm equivalent concrete. Apartments conditioned; stair/corridor spaces unconditioned. The PV over-roof remains an unheated shading element.
Ground boundary	Assumed constant ground-contact temperature of 10.2°C, based on the annual mean outdoor temperature.
Comfort setpoints	Heating 22°C; cooling 26°C. Cooling remains available when needed through the year; the May–September rule switches shading, not the cooling system.
Apartment air exchange	Fixed 0.5 ACH outdoor-air allowance, implemented through Ideal Loads; no separate infiltration, heat recovery or ventilation-fan electricity.
Corridor infiltration	Unconditioned stair and circulation spaces have no additional ventilation or infiltration allowance.
Dynamic glazing	U = 1.1 W/m²K in both states. SHGC 0.50 from 1 October to 30 April; 0.30 from 1 May to 30 September. Visible transmittance retained at 0.60.
Internal loads and DHW	Efficient appliances and cooking: 36.0 MWh/year, implemented as approximately 3.7 W/m² with the retained use schedule. Apartment lighting: 5 W/m². 80 residents; DHW approximately 40 L/person/day at 55°C. Appendix E documents appliance assumptions.

Component	Adopted treatment
Heat-pump post-processing	Outdoor-temperature-dependent performance; 40°C heating-water and 7°C chilled-water references, 55°C DHW, and 0.91 delivery allowance with an explicit load boundary.
Reporting	Hourly heating, cooling, hot-water, appliance and lighting outputs. Thermal services converted to electricity separately.

The ground-contact boundary is represented by a constant 10.2°C, calculated from the annual mean outdoor temperature in the Kyiv weather file. Apartments use heating and cooling setpoints of 22°C and 26°C, with year-round availability.

Seasonal solar control is represented by an effective SHGC of 0.30 from May to September and 0.50 from October to April. Both states retain U = 1.1 W/m²K and visible transmittance 0.6. Windows and glazed balcony doors switch together. The lower summer value represents the effect of blinds or shading on solar admission without prescribing a specific blind product.

Apartment ventilation is represented by an allowance of 0.5 air changes per hour (ACH), without heat recovery or ventilation-fan electricity. No separate infiltration allowance is added.

Solar shading is calculated using PixelCounting, with the balconies and roof shading elements included.

The household package includes one efficient fridge-freezer, dishwasher and washing machine per apartment, electric cooking, entertainment and small devices. Laundry is air-dried. Appliance-use assumptions follow the Passive House Institute (2023, Table 9, p. 81); efficient product data replace its fridge-freezer, dishwasher and washing-machine consumption defaults (Bosch, n.d.; European Commission, n.d.-c, n.d.-d). Appendix E sets out the quantities, use assumptions, product identifiers and annual calculation.

The resulting appliance and cooking allowance is 36.0 MWh/year, or 1,198.4 kWh per apartment per year. The annual allowance follows PHI usage assumptions and selected product data; its hourly distribution follows the retained apartment equipment schedule. It is applied through a design equipment density of approximately 3.7 W/m² and the retained daily schedule, equivalent to 5,763.4 full-load hours per year. The thermal calculation therefore reflects the lower heat released indoors by efficient appliances. Apartment and communal lighting remain a separate 7.4 MWh/year.

Efficient appliances form part of the proposed renovation, alongside the envelope and building services. This integrated approach is also explored by Abdulfattah, Fikry and

Hamed (2025) for a residential building in Cairo; the numerical appliance allowance here is derived from the PHI and product sources listed in Appendix E.

5.3 Hourly thermal demand and heat-pump electricity

EnergyPlus 25.1 uses the Kyiv station 333450 TMYx weather file, assembled from 2011–2025 data (Climate.OneBuilding.Org, n.d.). Its 8,760-hour sequence represents a typical year. The final annual calculation uses the revised appliance allowance; heating, cooling, hot water and lighting retain the other adopted settings.

Heating and cooling outputs include space conditioning and the treatment of incoming ventilation air. Hot-water demand is the heat delivered to water use. These thermal demands are converted to electricity in a separate hourly calculation after the EnergyPlus run; appliances and lighting are included directly as electrical consumption.

For each hour t, thermal demand Q is divided by the relevant heat-pump coefficient and the assumed delivery efficiency $\eta = 0.91$. Heating uses a 40°C water-supply temperature, hot water 55°C and cooling a 7°C chilled-water temperature. T_{out} denotes the hourly outdoor dry-bulb temperature from the same weather file. The equations give electricity E in kWh when Q is expressed in kWh:

$$E_{h,t} = \frac{Q_{h,t}}{COP_{h,t} \cdot \eta} \; ; \quad E_{c,t} = \frac{Q_{c,t}}{EER_{c,t} \cdot \eta} \; ; \quad E_{DHW,t} = \frac{Q_{DHW,t}}{COP_{DHW,t} \cdot \eta}$$

$$COP(\Delta T) = 6.81 - 0.121\,\Delta T + 0.000630\,\Delta T^2$$

Heating uses $\Delta T = 40 - T_{out}$ and hot water $\Delta T = 55 - T_{out}$, with temperature differences expressed in kelvin. The air-source COP relationship is attributed to Staffell et al. (2012) and reproduced by Thomassen et al. (2024, p. 12). Cooling uses $\Delta T = T_{out} - 7$; EER is linearly interpolated between the approximate points in Appendix B, read from the curve published by Ounis et al. (2022). Both coefficients vary hour by hour with outdoor temperature.

An overall efficiency of 0.91 is assumed for distribution, emission and control, using the value reported by Ounis et al. (2022). Hourly thermal demand is divided by the temperature-dependent COP or EER and by this efficiency to account for the additional electricity associated with delivering the required heating or cooling. The same efficiency allowance is applied to domestic hot water. The resulting values represent electricity consumption.

Annual electricity is the sum of the hourly service electricity, appliance consumption and lighting. Appendix B records the performance-curve limits and monthly results. For climate context, the same weather file gives 3,764.4 heating degree days at a 20°C base, calculated from daily mean temperatures.

$$E_{total} = E_{equipment} + E_{lighting} + E_h + E_c + E_{DHW}$$

5.4 Thermal demand and internal heat gains

Table 5.3 Annual thermal demands and heat-gain diagnostics.

Quantity	MWh/year	Meaning
Heating	67.5	Supply-air thermal demand
Cooling	14.3	Supply-air thermal demand
Hot water	56.2	Water-use thermal demand
Occupant gains	45.5	Heat released by people
Transmitted solar	35.9	Solar heat-gain diagnostic

The retrofit requires 67.5 MWh/year for heating, 14.3 MWh/year for cooling and 56.2 MWh/year for hot water. Heating is concentrated in winter; 99.4% of cooling occurs from May to September, with a July maximum of 6.1 MWh. Hot-water demand continues throughout the year.

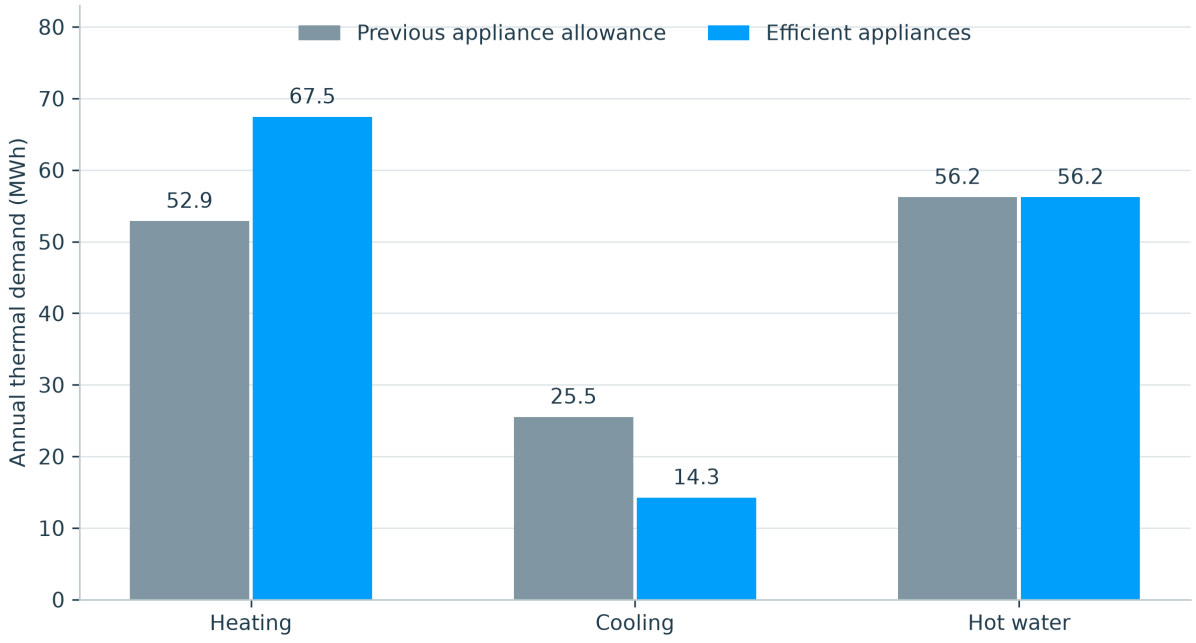

Figure 5.1 Effect of the efficient-appliance package on annual thermal demand. Both runs use the same envelope, weather, ventilation, seasonal glazing and shading settings; only the apartment appliance allowance changes. Source: EnergyPlus runs before and after the appliance revision.

Reducing appliance electricity from 65.2 to 36.0 MWh/year also reduces indoor heat gains. Heating demand consequently rises from 52.9 to 67.5 MWh/year, while cooling falls from 25.5 to 14.3 MWh/year, a reduction of 44.2%. Hot-water demand is unchanged. The differences between these two runs result from lower appliance heat gains; the seasonal solar-control settings remain unchanged.

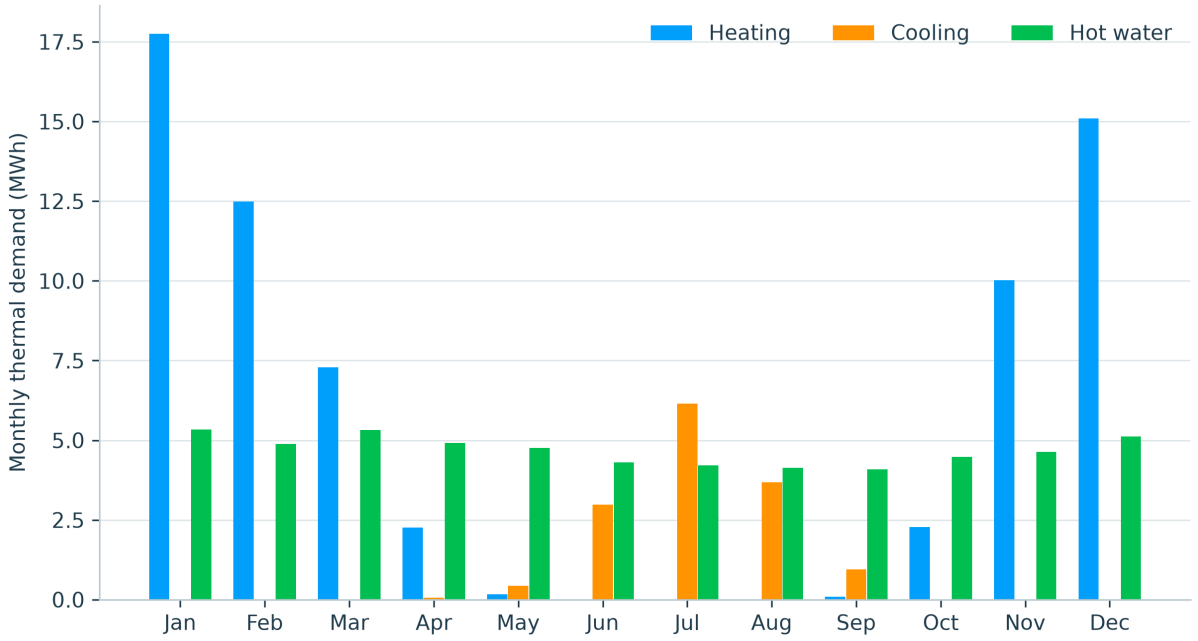

Figure 5.2 Monthly heating, cooling and hot-water thermal demand. Source: final EnergyPlus hourly outputs.

Table 5.4 Monthly thermal demand (MWh). Totals use unrounded hourly data.

Month	Heating	Cooling	Hot water
Jan	17.8	0.0	5.3
Feb	12.5	0.0	4.9
Mar	7.3	0.0	5.3
Apr	2.3	0.1	4.9
May	0.2	0.4	4.8
Jun	0.0	3.0	4.3
Jul	0.0	6.1	4.2
Aug	0.0	3.7	4.1

Month	Heating	Cooling	Hot water
Sep	0.1	0.9	4.1
Oct	2.3	0.0	4.5
Nov	10.0	0.0	4.6
Dec	15.1	0.0	5.1
Annual	67.5	14.3	56.2

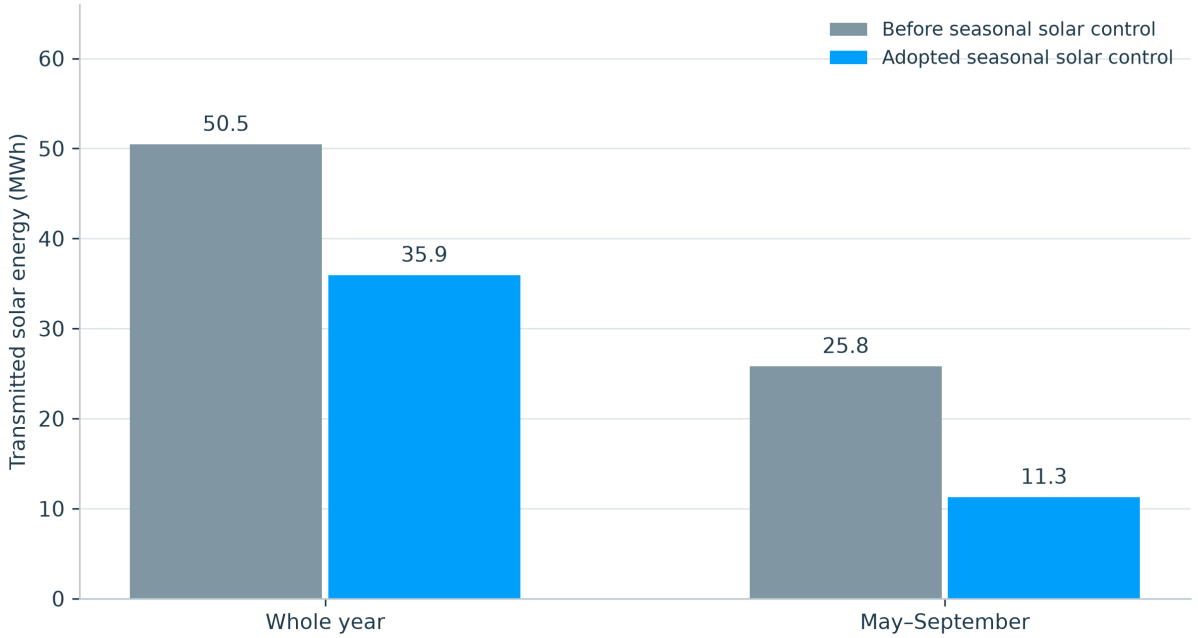

Figure 5.3 Transmitted solar energy in the earlier diagnostic and the adopted retrofit. The earlier values are taken from archived diagnostic results; the adopted values come from the final EnergyPlus run. Values represent solar energy admitted through glazing.

Annual transmitted solar radiation is 35.9 MWh, including 11.3 MWh from May to September. The lower summer SHGC reduces solar admission while the higher winter value retains useful heat gains. The appliance revision does not change transmitted solar energy; it changes the separate internal-gain contribution.

5.5 Annual and monthly electricity demand

Table 5.5 Annual electricity by end use and conditioned reference area. Heating, cooling and hot water include the hourly heat-pump conversion; lighting includes communal spaces. Totals use unrounded values;

End use	MWh/year	kWh/m²/year
Appliances and cooking	36.0	21.2
Lighting	7.4	4.3
Heating	24.9	14.7
Cooling	4.7	2.8
Hot water	24.2	14.3
Total	97.1	57.2

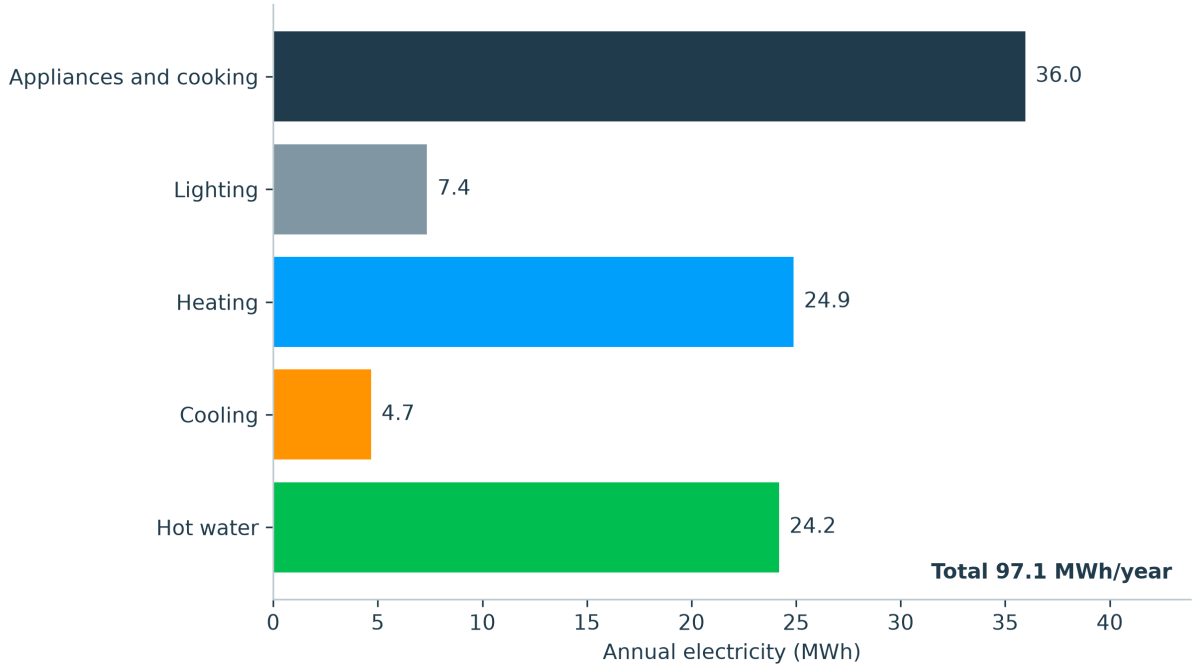

Figure 5.4 Annual electricity consumption by use. Heating, cooling and hot water are derived from hourly thermal demand and temperature-dependent performance; appliances, cooking and lighting come from EnergyPlus. Source: author's calculations.

Total electricity is 97.1 MWh/year, or 57.2 kWh/m²/year. Appliances and cooking account for 36.0 MWh and lighting for 7.4 MWh; heating, cooling and hot water require a further 53.7 MWh. Appliance and lighting electricity together equal 25.5 kWh/m²/year.

Heating, cooling and hot-water electricity are calculated hour by hour using COP and EER values that vary with outdoor temperature. The resulting effective annual performance ratios are approximately 3.0 for heating, 3.3 for cooling and 2.6 for hot water, before the delivery allowance. Each ratio is annual thermal demand divided by the corresponding electricity before that allowance. January has the highest total electricity demand at 13.7 MWh. July requires 7.0 MWh, including 2.0 MWh for cooling.

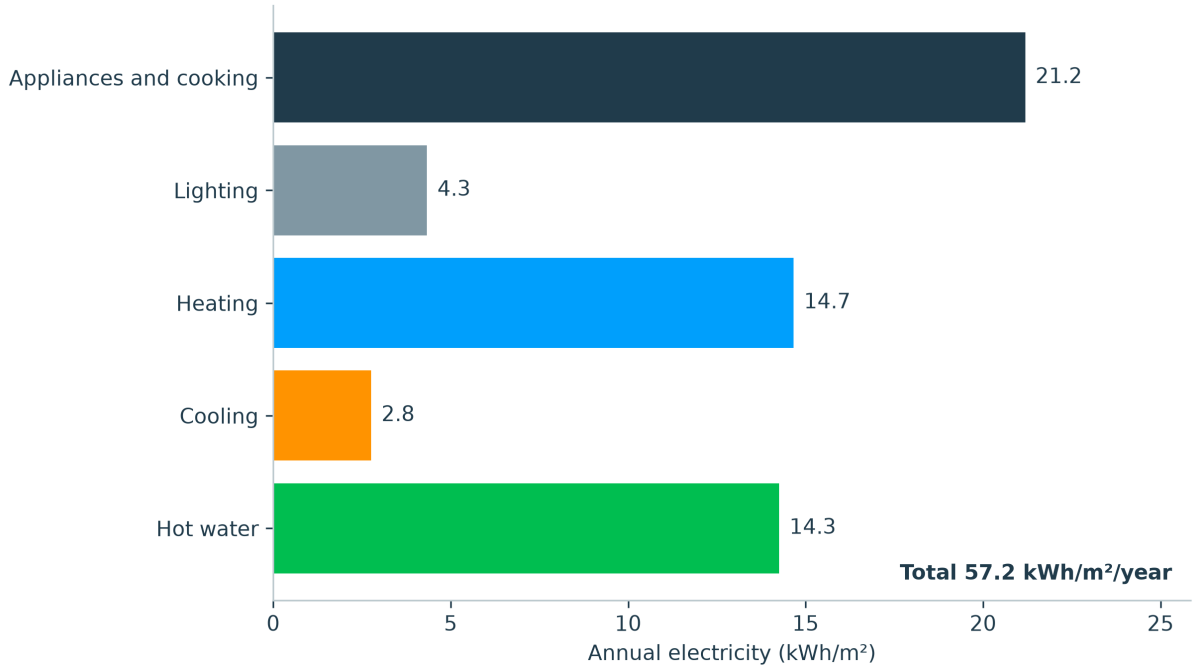

Figure 5.5 Annual electricity per square metre of conditioned reference area. All end uses share the 1,697.0 m² denominator; lighting includes communal spaces. Source: author's calculations.

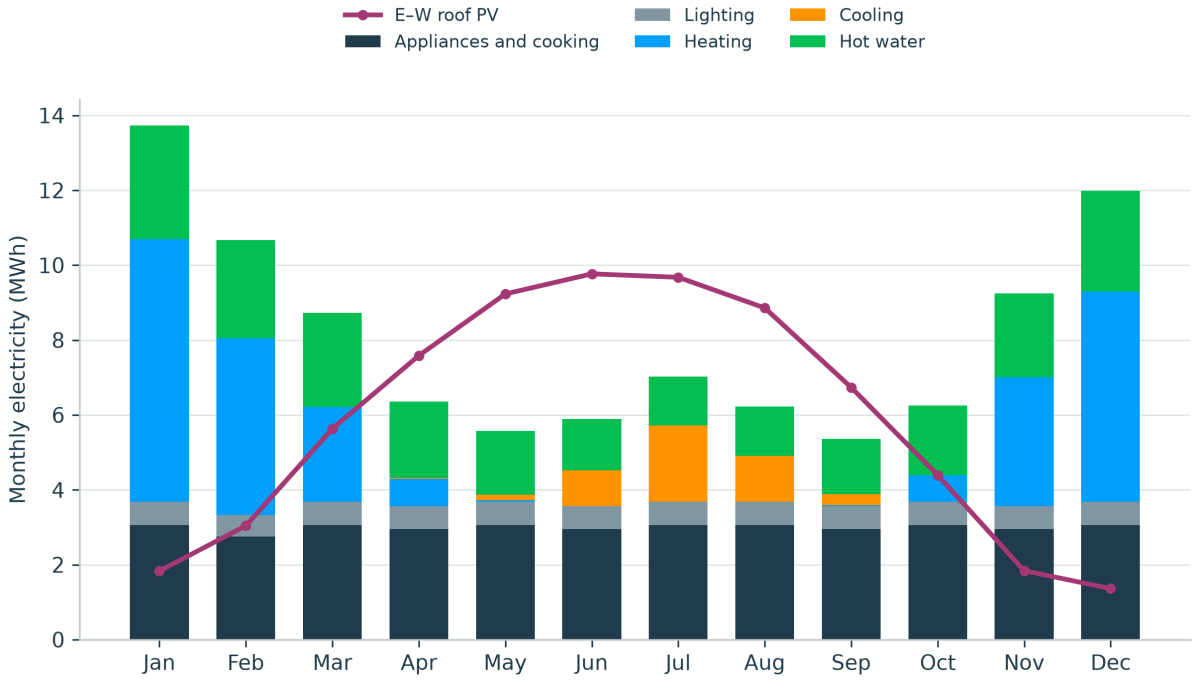

Figure 5.6 Monthly electricity demand by use and east–west redesigned-roof PV generation. EnergyPlus and PVGIS represent separate typical-climate calculations; monthly comparisons do not establish hourly coincidence.

5.6 PV generation relative to retrofit electricity

The three redesigned roofs are compared with the same 97.1 MWh annual electricity demand. This provides a common reference for their different generating capacities; separate thermal runs would be needed to quantify changes in demand caused by rotating the building.

Table 5.6 Redesigned-roof generation relative to the common annual retrofit electricity demand.

Roof orientation	PV MWh/year	PV / demand
N-S	67.8	69.9%
E-W	69.9	72.1%
SE-NW	67.6	69.6%

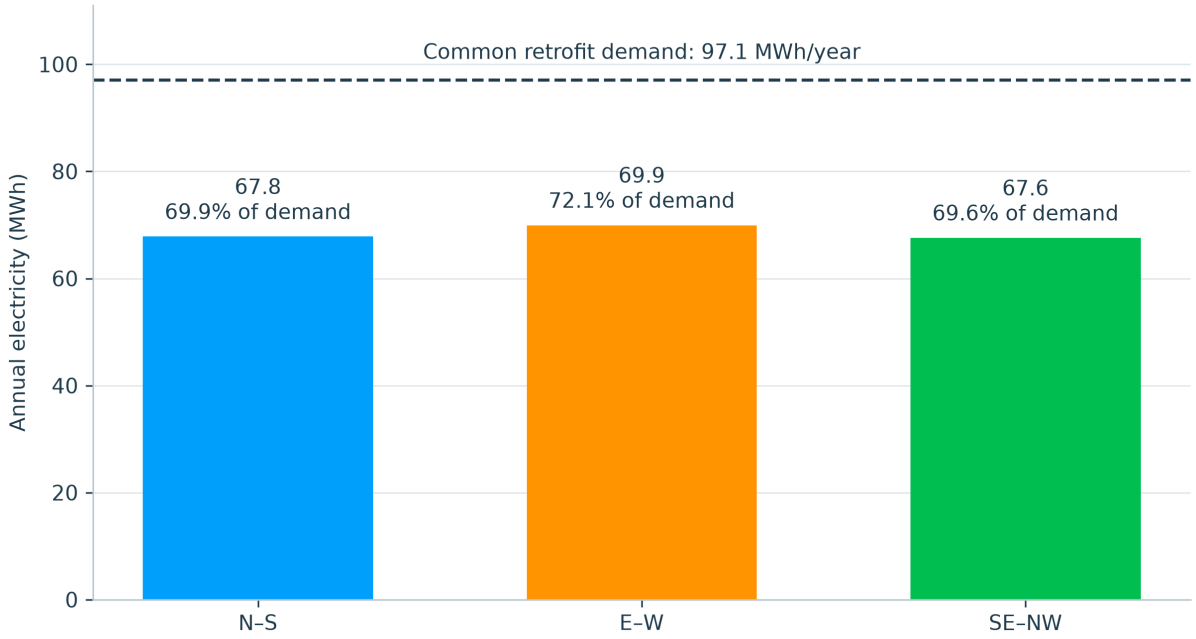

Figure 5.7 Annual PV generation relative to the common retrofit electricity demand. Percentages compare annual energy totals, not self-consumption.

The east–west roof produces 69.9 MWh/year, equivalent to 72.1% of annual electricity demand. The north–south and southeast–northwest roofs contribute annual equivalents of 69.9% and 69.6%. For the east–west case, annual demand exceeds PV generation by 27.1 MWh. Actual grid imports also depend on the timing of production and use.

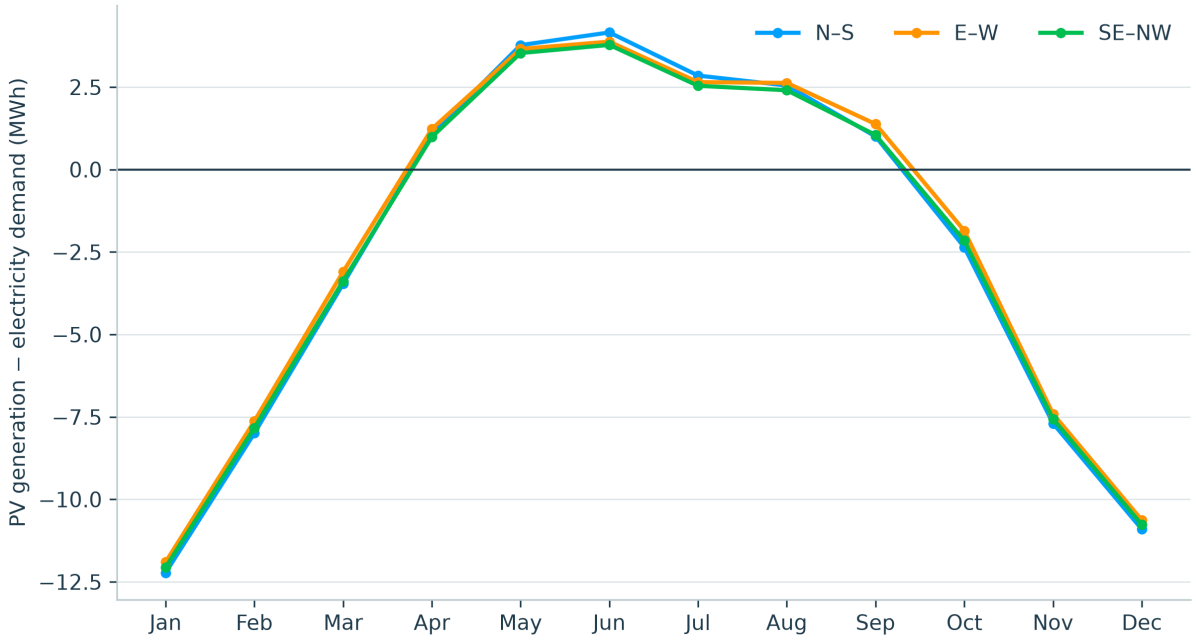

Figure 5.8 Monthly PV generation minus the common retrofit electricity demand. Positive values indicate a monthly energy excess, not measured export or hourly self-sufficiency.

For the east–west roof, monthly generation exceeds electricity demand from April to September. January combines low solar generation with the highest heating requirement. Matching hourly PV generation with hourly electricity demand would allow self-consumption and storage requirements to be assessed.

6 District rooftop PV potential and community energy

The rooftop strategies developed for the representative Khrushchevka building are applied to the selected Vidradnyi area in Kyiv to estimate their collective generation potential. The assessment includes 63 residential roof units and yields approximately 12.6 GWh of electricity per year. This provides the basis for discussing a renewable energy community (REC) and the spatial organisation of shared energy services.

The representative building provides a consistent basis for comparing rooftop PV strategies. At microdistrict scale, the strategies adapt to each roof's dimensions and orientation.



Figure 6.1 Location of the Vidradnyi study area within Kyiv. Source: Apple Maps; author's location annotation.

Table 6.1 Scope of the district assessment.

Study area	Assessed roof units	Other buildings retained as context
57.8 ha	63	71





Figure 6.2 Vidradnyi study area in satellite imagery (above) and assessed roof-unit identifiers (below). Grey footprints are outside the generation assessment (OpenStreetMap contributors, 2026). Satellite imagery: Apple Maps; assessment map: author, using OpenStreetMap data.

6.1 Study area and roof units

The assessment includes elongated residential blocks compatible with the reference building's roof strategies. Their roof units are evaluated using one common generation method. The boundary is an analytical study area, rather than a verified administrative microdistrict (OpenStreetMap contributors, 2026).

A straight block forms one roof unit. Each substantial wing of an L-shaped configuration is a separate unit with its own numeric ID. Small end returns in 003, 030, 033 and 119 are represented by straight rectangles preserving the mapped plan area and main-axis length. The existing pitched or flat roof is replaced by the proposed surface in this retrofit scenario.

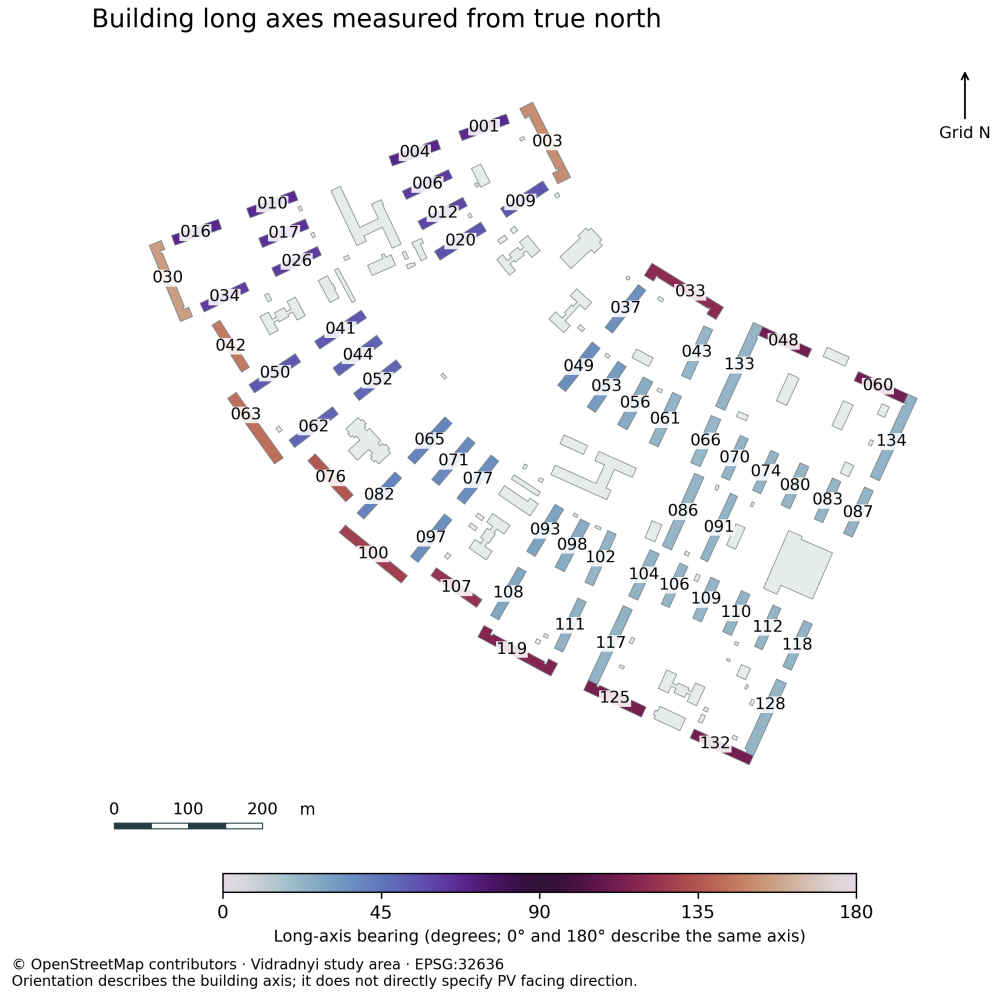

Figure 6.3 Measured long-axis bearings, clockwise from true north. Calculations use these bearings directly rather than assigning the nearest reference orientation.

6.2 Adapting the roof strategy

The dominant long edge defines each unit's axis; length and width are measured along and across it in QGIS. Both reference-derived roof forms were compared using the same panel-fitting and generation method: a slope along the length (L) and a slope across the width (T). T produced the higher estimated annual output on all 63 units; the complete comparison is recorded in Appendix D, Schedule D.2.

The selected transverse surface faces the more southerly side of each block. Its reference tilt of 15° is reduced only where necessary to respect the 3 m maximum rise, giving adopted tilts of 11.4° to 15°. This adjusts the architectural strategy to the actual roof width while retaining a continuous surface.

Full 1.800 × 1.134 m modules are fitted to the inclined surface with 20 mm gaps and a 0.50 m perimeter setback. Both module rotations and alternative grid positions are tested. The fitted count is multiplied by the reference retention fraction 132/145 and rounded down to whole modules. This corresponds to an approximately 9.0% allowance for roof services. Each module contributes 0.505 kWp. The fraction comes from the reference layout, where 132 modules occupy 145 unobstructed grid positions; district obstructions are represented by this common allowance.

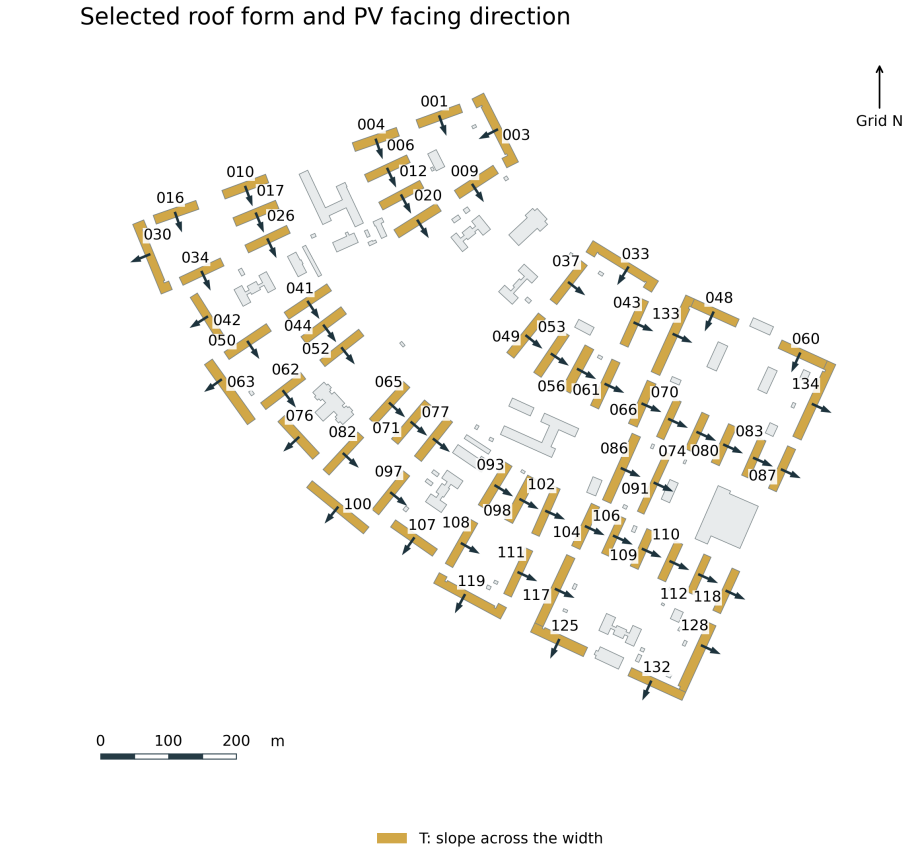

Figure 6.4 Selected transverse roofs and PV facing directions.

6.3 Estimated electricity generation

PVGIS 5.3 supplies annual and monthly generation per installed kWp for each adapted tilt and facing direction. Requests use the district location 50.4278° N, 30.4223° E, SARAH3 radiation data, crystalline-silicon modules, free-standing mounting, a terrain horizon and 14% system losses. Multiplying these outputs by the fitted array capacity gives each roof's generation (European Commission Joint Research Centre, n.d.-a).

Table 6.2 Combined generation from the 63 assessed roof units.

PV modules	Installed capacity MWp	Annual generation GWh
24,972	12.6	12.6

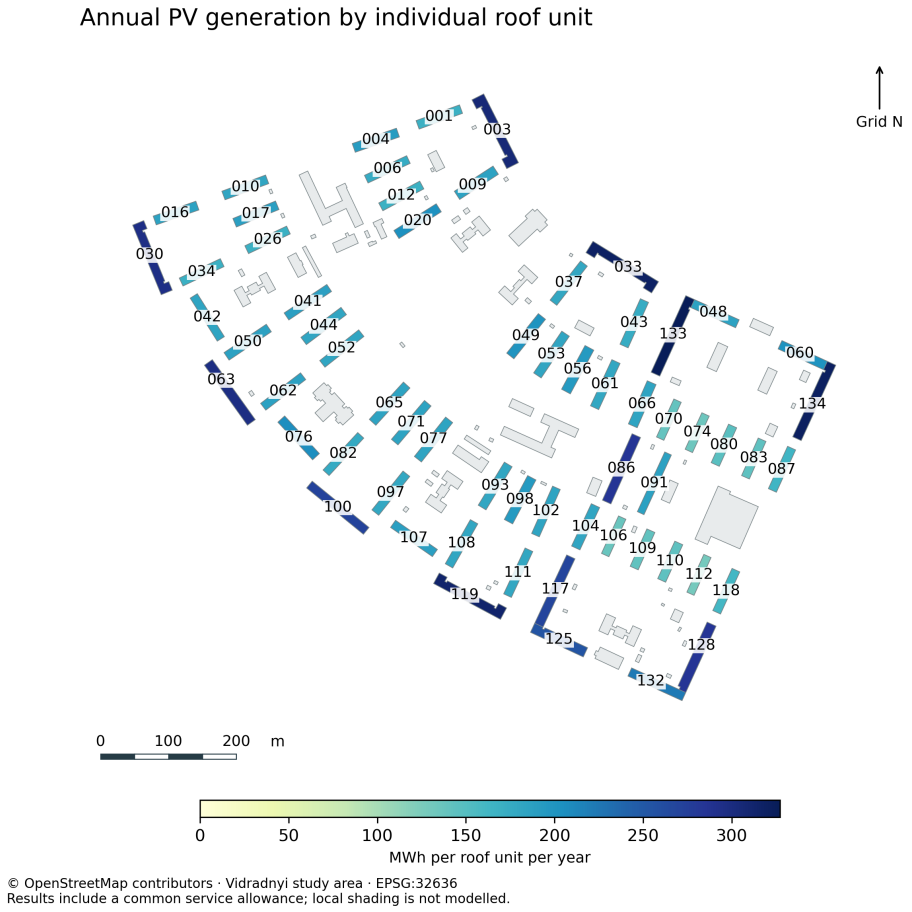

Figure 6.5 Estimated annual electricity generation per assessed roof unit. Each wing is mapped separately, so every colour corresponds to one calculation unit.

Units 086 and 091 have similar orientations, but 086 is wider and longer, accommodates more panels and therefore generates more electricity (Appendix D, Schedule D.1).

The combined total is the potential of the selected residential roofs within the study boundary. It demonstrates the scale achieved by repeating the retrofit strategy at microdistrict scale. Appendix D, Schedule D.1 links every mapped ID to its roof geometry, panel count, installed capacity and generation.

6.4 Reading the spatial results

Annual production depends on both array size and productivity. Specific yield, expressed in kWh per installed kWp, isolates the effect of adapted tilt and facing direction. Across the selected roofs it ranges from 971.3 to 1,034.3 kWh/kWp/year. Larger total contributions therefore do not necessarily indicate a more productive orientation.

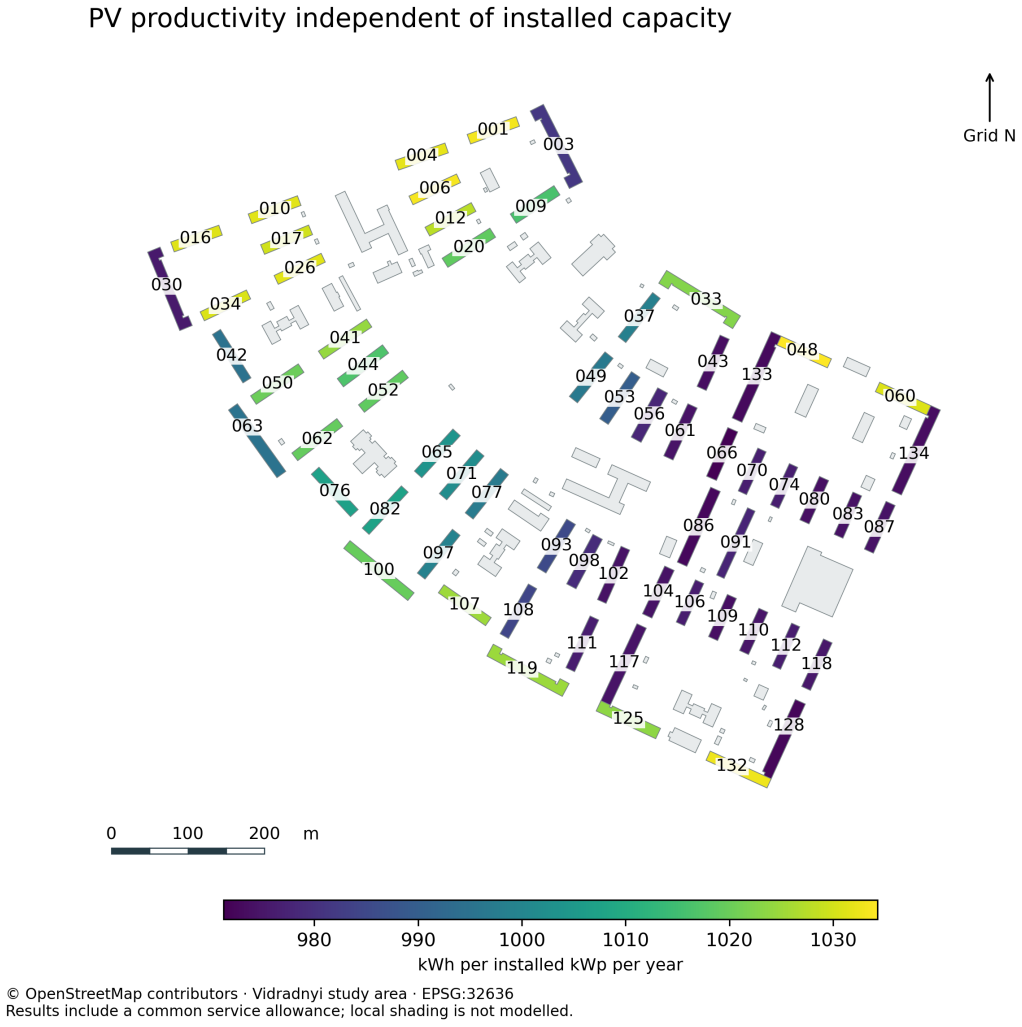

Figure 6.6 Annual PV productivity per installed kWp. Read alongside Figure 6.5 to distinguish solar performance from array size.

6.5 Seasonal supply and collective use

Approximately 75.6% of annual generation occurs from April to September. June contributes about 1.8 GWh, compared with 0.2 GWh in December. The concentration in warmer months is a defining characteristic of this collective resource: annual generation does not represent a constant supply.

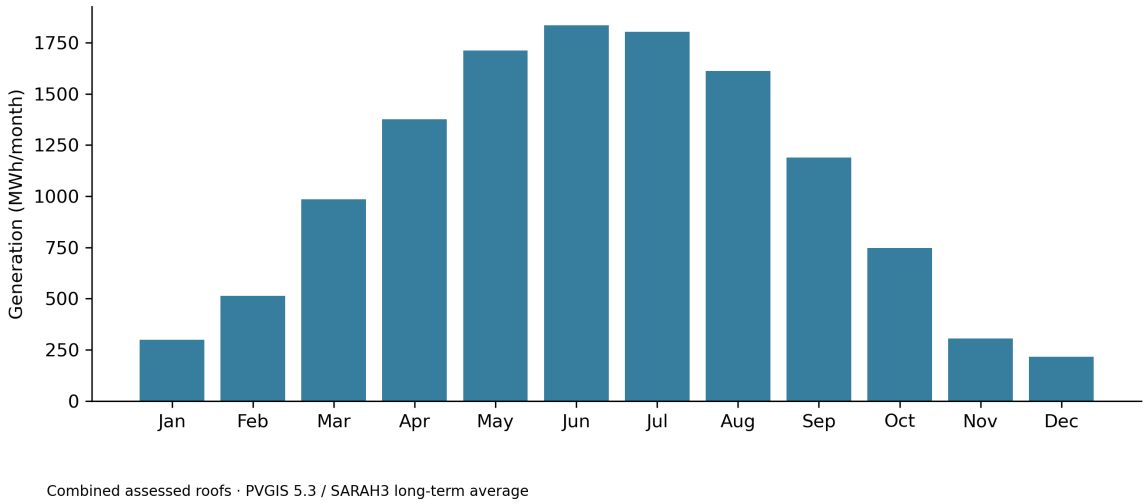

Figure 6.7 Combined monthly generation from the selected roofs. Values are long-term PVGIS averages, rather than a forecast for a particular year.

A renewable energy community offers an organisational framework through which residents could coordinate investment, operation and the allocation of locally generated electricity. The European community-energy model provides a conceptual reference for this discussion; a Kyiv project would require a locally applicable participation and market arrangement (European Commission, n.d.-a).

For Vidradnyi, a grid-connected collective arrangement is the proposed starting point. Electricity could serve participating households and shared building services when production and use coincide; the grid could receive available exports and supply electricity at other times. Metering and agreed allocation rules would connect individual roof contributions to collective benefits. The estimated generation is the supply resource, not a calculated surplus or an amount already available for export.

Table 6.3 Options for organising the collective resource.

Option	Purpose	Architectural implication
Grid-connected sharing	Coordinate generation and consumption across participants	Metering, inverter space and accessible connections

Option	Purpose	Architectural implication
Building or cluster batteries	Shift some daytime production to later use	Distributed equipment spaces and maintenance access
Shared central battery	Pool storage under one operating arrangement	A dedicated accessible facility and connection route

6.6 Spatial implications and storage

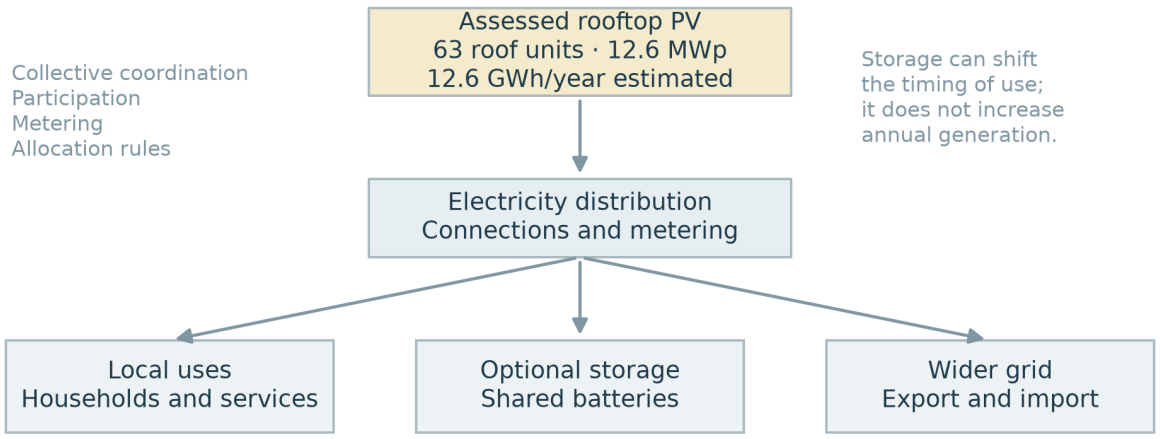

Figure 6.8 Conceptual collective-energy arrangement. Arrows represent possible electricity flows; the diagram does not locate equipment or prescribe network routes.

Across Vidradnyi, rooftop renovation could become a shared energy project, linking improvements to individual buildings with the renewal of the wider microdistrict. The proposed roofs offer an estimated annual PV generation of 12.6 GWh. Repeated building types make it possible to introduce the intervention gradually, building by building or in groups, while maintaining a common approach to roof design and technical systems. Courtyards and communal landscapes should remain spaces for everyday life, with energy equipment accommodated in suitable service areas.

Storage introduces a further architectural choice: equipment could be distributed among buildings or concentrated in a shared facility. Building or cluster batteries could serve smaller groups of properties, while a central installation would require accessible technical premises with sufficient space for connections and maintenance. These options describe possible ways of organising the infrastructure; no battery location has been selected (European Commission, n.d.-b).

The concentration of generation in summer also makes the timing of electricity use important. Shared activities and services operating during daylight hours could use part of the output directly, while batteries could store some daytime generation for evening use. Daily battery storage, however, would not transfer the summer surplus into winter. The monthly results reveal this seasonal pattern; storage capacity and the balance between direct use, imports and exports would require matching hourly generation with consumption.

Heat pumps offer another connection between rooftop electricity and residential renewal. PV generation could contribute to domestic hot-water production and, within

a future collective system, to space heating. Chapter 5 demonstrates how temperature-dependent heat-pump performance links thermal demand to electricity consumption. At microdistrict scale, the contribution to heat supply would depend on the demand profile, equipment and thermal infrastructure (IEA, 2022).

The estimated 12.6 GWh/year represents the microdistrict's rooftop generation potential. It includes terrain-horizon effects but excludes shading from nearby buildings and rooftop obstructions (European Commission Joint Research Centre, n.d.-b). Comparing this resource with collective electricity demand would establish how much could be used locally and inform the organisation of shared energy services.

7 Conclusion

Rooftop photovoltaics offer a way to connect the renewal of Kyiv's Khrushchevka housing with local electricity generation. Under the common photovoltaic assumptions, roof geometry and the number of modules accommodated determine the differences in annual generation between the tested configurations. A continuous inclined roof produces more annual electricity than every rack layout tested, while allowing the design to respond to each building's orientation.

Across the three orientations, the conventional racks generate 23.1–45.6 MWh/year, while the redesigned roofs reach 67.6–69.9 MWh/year. The 35° racks achieve the highest yield per installed kilowatt, but their row spacing reduces the number of modules that fit. The continuous roofs accommodate more modules and therefore produce more electricity overall. East–west achieves the highest annual generation at 69.9 MWh/year, followed by north–south at 67.8 MWh/year and southeast–northwest at 67.6 MWh/year. This narrow range supports a roof strategy that can adapt its inclination and module orientation to the dimensions and alignment of the assessed buildings.

For the scenario without the wider energy retrofit, the adopted historical household and communal electricity benchmark is 63.4 MWh/year for 30 apartments. It combines the Ukrainian household statistic with an estimated allowance for communal lighting (Section 5.1; State Statistics Service of Ukraine, n.d.). Annual generation from the rack layouts is equivalent to 36.4–71.9% of this benchmark. The redesigned roofs generate an annual quantity equivalent to 106.6–110.4% of the adopted electricity benchmark, with district heating and central hot water remaining outside this comparison.

The deep retrofit combines envelope upgrades, solar control, more efficient appliances and heat pumps replacing the existing thermal supply. Its annual electricity demand is 97.1 MWh/year, equivalent to 57.2 kWh/m²/year. The redesigned roofs generate an annual quantity equivalent to 69.6–72.1% of this demand. The retrofit total includes heat-pump electricity for heating and hot water, alongside cooling, efficient appliances and lighting. The two scenarios therefore differ in both energy supply and demand assumptions, so their electricity totals cannot be used to calculate total energy savings.

The appliance revision also shows why household electricity and thermal demand should be considered together. More efficient appliances reduce direct consumption and the heat released indoors. This lowers cooling demand but increases winter heating demand. Accounting for these interactions, together with heat-pump performance that varies with outdoor temperature, provides a consistent estimate of the proposed electrified building. Roof generation and demand reduction can therefore be evaluated as connected parts of residential renovation.

Seasonal timing remains important even where annual generation exceeds annual demand. The east–west roof generates more electricity than the retrofit requires in each month from April to September, while demand exceeds generation during the remaining months. An annual ratio above 100% therefore does not establish continuous self-sufficiency. These results support a grid-connected approach that prioritises direct use of solar electricity and aligns consumption with generation where possible. Storage capacity would need to be assessed against the hourly timing of surplus and shortfall.

Across the 63 residential roof units of Vidradnyi, the estimated installed capacity is 12.6 MWp and annual generation is 12.6 GWh, with 75.6% produced between April and September. The mapped potential is distributed across existing buildings, allowing renewable generation to expand without occupying open communal ground. The assessment demonstrates how the roof strategy can be adapted to the dimensions and orientations of the assessed Vidradnyi roof units. This spatial distribution provides a basis for coordinating rooftop generation within a renewable energy community.

Further development would match this generation potential to hourly demand across the microdistrict and assess local shading, structural capacity and roof construction. These steps would inform installation priorities, electricity-sharing arrangements and storage requirements. At building scale, the redesigned roofs produce an annual quantity greater than the historical electricity benchmark or equivalent to around seven-tenths of the fully electrified retrofit demand. At the scale of Vidradnyi, the same architectural approach connects residential renewal with a collective solar resource.

References

Abdulfattah, H.A.M., Fikry, A.A. and Hamed, R.E. (2025) 'Passive House-based energy efficiency design criteria: a case study of a residential building in Cairo', *Open House International*, 50(1), pp. 118–138. doi: 10.1108/OHI-02-2024-0045.

Aguacil, S., Lufkin, S. and Rey, E. (2019) 'Active surfaces selection method for building-integrated photovoltaics (BIPV) in renovation projects based on self-consumption and self-sufficiency', *Energy and Buildings*, 193, pp. 15–28. doi: 10.1016/j.enbuild.2019.03.035.

Apple Maps (n.d.) *Satellite imagery of Kyiv and Vidradnyi*. Images supplied by the author; acquisition date unavailable. Location annotations by the author.

Aste, N., Caputo, P., Del Pero, C., Ferla, G., Huerto-Cardenas, H.E., Leonforte, F. and Miglioli, A. (2020) 'A renewable energy scenario for a new low carbon settlement in northern Italy: Biomass district heating coupled with heat pump and solar photovoltaic system', *Energy*, 206, 118091. doi: 10.1016/j.energy.2020.118091.

Aste, N., Del Pero, C., Leonforte, F., Ounis, S. and Abdelrahim, A.M.G. (2024) 'The role of photovoltaic technology in achieving net zero energy target in residential buildings', *Energy Strategy Reviews*, 55, 101543. doi: 10.1016/j.esr.2024.101543.

Bham, S., Chesnoiu, G., Gschwind, B., Eissa, Y. and Blanc, P. (2025) *GTI schematic*. Wikimedia Commons, CC BY 4.0. Available at: Wikimedia Commons (Accessed: 21 August 2026).

Bosch (n.d.) *KGN39OXBT freestanding fridge-freezer: product specification*. Available at: Bosch product specification (Accessed: 22 September 2026).

Byrne, J., Taminiau, J., Kim, K.N., Seo, J. and Lee, J. (2016) 'A solar city strategy applied to six municipalities: integrating market, finance, and policy factors for infrastructure-scale photovoltaic development in Amsterdam, London, Munich, New York, Seoul, and Tokyo', *Wiley Interdisciplinary Reviews: Energy and Environment*, 5(1), pp. 68–88. doi: 10.1002/wene.182.

Camarasa, C. et al. (2022) 'A global comparison of building decarbonization scenarios by 2050 towards 1.5–2°C targets', *Nature Communications*, 13, 3077. doi: 10.1038/s41467-022-29890-5.

City of Freiburg (n.d.) *Quartier Vauban: nachhaltiges Wohnen*. Available at: City of Freiburg (Accessed: 19 August 2026).

Climate.OneBuilding.Org (n.d.) *Kyiv station 333450 TMYx weather data, 2011–2025*. File: UKR_KC_Kyiv.333450_TMYx.2011-2025.epw. Available at: Climate.OneBuilding.Org (Accessed: 22 September 2026).

Compagnon, R. (2004) 'Solar and daylight availability in the urban fabric', *Energy and Buildings*, 36(4), pp. 321–328. doi: 10.1016/j.enbuild.2004.01.009.

Constantinou, S., Al-naemi, F., Alrashidi, H., Mallick, T. and Issa, W. (2024) 'A review on technological and urban sustainability perspectives of advanced building-integrated photovoltaics', *Energy Science & Engineering*, 12(3), pp. 1265–1293. doi: 10.1002/ese3.1639.

Del Pero, C., Aste, N., Leonforte, F. and Sfolcini, F. (2023) 'Long-term reliability of photovoltaic c-Si modules – A detailed assessment based on the first Italian BIPV project', *Solar Energy*, 264, 112074. doi: 10.1016/j.solener.2023.112074.

Del Pero, C., Leonforte, F. and Aste, N. (2024) 'Building-Integrated Photovoltaics in Existing Buildings: A Novel PV Roofing System', *Buildings*, 14(8), 2270. doi: 10.3390/buildings14082270.

Duffie, J.A. and Beckman, W.A. (2013) *Solar Engineering of Thermal Processes*. 4th edn. Hoboken, NJ: Wiley.

European Commission (2019) *Commission Delegated Regulation (EU) 2019/2014 of 11 March 2019 with regard to energy labelling of household washing machines and household washer-dryers*. Annex IV; consolidated text of 1 May 2021. Available at: EUR-Lex (Accessed: 22 August 2026).

European Commission (n.d.-a) *Energy communities*. Directorate-General for Energy. Available at: Energy communities (Accessed: 21 September 2026).

European Commission (n.d.-b) *Energy storage*. Directorate-General for Energy. Available at: Energy storage (Accessed: 21 August 2026).

European Commission (n.d.-c) *EPREL product information sheet: Bosch SMV4ECX28E household dishwasher, registration 1961923*. Available at: EPREL dishwasher record (Accessed: 22 August 2026).

European Commission (n.d.-d) *EPREL product information sheet: Haier HW80-BP1439N household washing machine, registration 339290*. Available at: EPREL washing-machine record (Accessed: 22 August 2026).

European Commission Joint Research Centre (n.d.-a) *PVGIS 5 user manual and non-interactive API documentation*. Available at: PVGIS user manual and API documentation (Accessed: 21 August 2026).

European Commission Joint Research Centre (n.d.-b) *PVGIS horizon profile*. Available at: Horizon profile (Accessed: 21 September 2026).

Freitas, S., Catita, C., Redweik, P. and Brito, M.C. (2015) 'Modelling solar potential in the urban environment: State-of-the-art review', *Renewable and Sustainable Energy Reviews*, 41, pp. 915–931.

Hobhouse, C. (2025) 'Keeping the lights on: How Ukraine can build a resilient energy system (and why this matters to the EU)', *European Union Institute for Security Studies*, 28 March. Available at: EUISS commentary.

IEA (2022) *The Future of Heat Pumps*. Paris: International Energy Agency. Available at: The Future of Heat Pumps (Accessed: 22 September 2026).

IEA (2024a) *Ukraine's Energy Security and the Coming Winter*. Paris: International Energy Agency. Available at: Ukraine's Energy Security and the Coming Winter (Accessed: 19 September 2026).

IEA (2024b) *Empowering Ukraine Through a Decentralised Electricity System*. Paris: International Energy Agency. Available at: Empowering Ukraine Through a Decentralised Electricity System (Accessed: 19 September 2026).

IEA (2025) *Policy Options to Accelerate Distributed Solar PV in Ukraine*. Paris: International Energy Agency. Available at: Policy Options to Accelerate Distributed Solar PV in Ukraine (Accessed: 24 August 2026).

IEA PVPS Task 15 (2018) *International definitions of BIPV*. Available at: International definitions of BIPV (Accessed: 19 September 2026).

IEA PVPS Task 15 (2023) *Fire Safety of BIPV: International Mapping of Accredited and R&D Facilities in the Context of Codes and Standards*. Report IEA-PVPS T15-15:2023. Available at: IEA PVPS report (Accessed: 24 August 2026).

IPCC (2022) 'Buildings', Chapter 9 in *Climate Change 2022: Mitigation of Climate Change. Contribution of Working Group III to the Sixth Assessment Report of the Intergovernmental Panel on Climate Change*. Cambridge: Cambridge University Press. Available at: IPCC Chapter 9 (Accessed: 19 September 2026).

IPCC (2023) *Climate Change 2023: Synthesis Report. Contribution of Working Groups I, II and III to the Sixth Assessment Report of the Intergovernmental Panel on Climate Change*. Geneva: IPCC. Available at: AR6 Synthesis Report (Accessed: 24 September 2026).

Jacobson, M.Z. and Jadhav, V. (2018) 'World estimates of PV optimal tilt angles and ratios of sunlight incident upon tilted and tracked PV panels relative to horizontal panels', *Solar Energy*, 169, pp. 55–66. doi: 10.1016/j.solener.2018.04.030.

Keramidas, K. et al. (2025) *Global Energy and Climate Outlook 2024: Updating NDCs and closing the ambition gap – indicators for 1.5°C alignment*. Luxembourg: Publications Office of the European Union. EUR 40173, JRC139986. doi: 10.2760/9028706.

KievZNIIEP (n.d.) *Passport of standard project 1-480A-31: Five-storey two-section large-panel residential building with 30 apartments*. Part 2, sheets 1–2, passport no. 016762. Project approved 20 November 1963 and introduced 23 March 1964. Scan supplied by the author.

Lindberg, F., Grimmond, C.S.B., Gabey, A., Huang, B., Kent, C.W., Sun, T., Theeuwes, N.E., Järvi, L., Ward, H.C., Capel-Timms, I., Chang, Y., Jonsson, P., Krave, N., Liu, D., Meyer, D.,

Olofson, K.F.G., Tan, J., Wästberg, D., Xue, L. and Zhang, Z. (2018) 'Urban Multi-scale Environmental Predictor (UMEP): An integrated tool for city-based climate services', *Environmental Modelling & Software*, 99, pp. 70–87. doi: 10.1016/j.envsoft.2017.09.020.

LONGi (n.d.) *Hi-MO X10 LR7-54HVH 480–505M: module specifications*. Model LR7-54HVH-505M, 505 Wp, 1800 × 1134 × 30 mm. Available at: LONGi module specifications (Accessed: 22 September 2026).

Lund, H., Werner, S., Wiltshire, R., Svendsen, S., Thorsen, J.E., Hvelplund, F. and Mathiesen, B.V. (2014) '4th Generation District Heating (4GDH): Integrating smart thermal grids into future sustainable energy systems', *Energy*, 68, pp. 1–11.

Microsoft (n.d.) *GlobalMLBuildingFootprints* [dataset]. GitHub. Available at: GlobalMLBuildingFootprints (Accessed: 24 August 2026).

NABCEP (2019) *PV Certification Study Guide*. Version 8. Edited by B. Brooks and B. Mehalic. Available at: NABCEP study guide (Accessed: 21 September 2026).

Ni, P. et al. (2025) 'Building integrated photovoltaics that move beyond rooftops', *Cell Reports Physical Science*, 6(8), 102725. doi: 10.1016/j.xcrp.2025.102725.

NOAA (n.d.) *General Solar Position Calculations*. Global Monitoring Laboratory. Available at: Solar position calculations (Accessed: 21 August 2026).

OpenStreetMap contributors (2026) *Building footprints and tags for Vidradnyi* [dataset]. Retrieved 19 September 2026. © OpenStreetMap contributors, ODbL. Available at: OpenStreetMap attribution and licence.

Ounis, S., Aste, N., Butera, F.M., Del Pero, C., Leonforte, F. and Adhikari, R.S. (2022) 'Optimal balance between heating, cooling and environmental impacts: a method for appropriate assessment of building envelope's U-value', *Energies*, 15(10), 3570. doi: 10.3390/en15103570.

Passive House Institute (2023) *Criteria for Buildings: Passive House – EnerPHit – PHI Low Energy Building*. Version 10c. Darmstadt: Passive House Institute. Section 2.5.11 and Table 9, p. 81. Available at: Criteria for Buildings, version 10c (Accessed: 22 September 2026).

Quaschning, V. (2016) *Understanding Renewable Energy Systems*. 2nd edn. Abingdon: Routledge.

Ruan, T., Laumert, B. and Wang, W. (2026) 'Techno-economic analysis of urban bifacial PV in high-latitude area', *Renewable Energy*, 258, 124916. doi: 10.1016/j.renene.2025.124916.

Sandia National Laboratories, PV Performance Modeling Collaborative (n.d.) *Plane of array irradiance*. Available at: Plane of array irradiance (Accessed: 19 September 2026).

Sengupta, M., Habte, A., Wilbert, S., Gueymard, C., Remund, J., Lorenz, E., van Sark, W. and Jensen, A. (eds) (2024) *Best Practices Handbook for the Collection and Use of Solar*

Resource Data for Solar Energy Applications. 4th edn. NREL/TP-5D00-88300; IEA-PVPS T16-10:2024. doi: 10.2172/2448063.

Shu, X., Zhu, J.J., Jiang, H. and Chen, S.Y. (2025) 'Scientometric analysis of building integrated photovoltaics research: development, themes, and main trends', *Journal of Asian Architecture and Building Engineering*, 24(6), pp. 5302–5334. doi: 10.1080/13467581.2024.2421263.

Shyrochyn, S. (2020) 'Усі свої: Як у київській міфології з'явилися «чешки» та «кубинські корпуси»', *Bird in Flight*, 8 May. Available at: Bird in Flight article (Accessed: 3 June 2026).

Staffell, I., Brett, D., Brandon, N. and Hawkes, A. (2012) 'A review of domestic heat pumps', *Energy & Environmental Science*, 5, pp. 9291–9306. doi: 10.1039/C2EE22653G.

State Statistics Service of Ukraine (n.d.) *SDG indicator 7.5.3: household electricity consumption*. Data for 2020. Available at: Indicator 7.5.3 (Accessed: 19 September 2026).

Thomassen, G., Fuhrmanek, A., Cadenovic, R., Pozo Camara, D. and Vitiello, S. (2024) *Redispatch and Congestion Management*. European Commission Joint Research Centre. EUR 31924 EN, JRC137685. doi: 10.2760/853898.

U.S. Department of Energy (2025) *EnergyPlus 25.1 Input Output Reference*. Sections ZoneHVAC and WaterUse. Available at: EnergyPlus documentation (Accessed: 22 August 2026).

U.S. Department of Energy (n.d.-a) *Solar photovoltaic cell basics*. Available at: Solar photovoltaic cell basics (Accessed: 19 August 2026).

U.S. Department of Energy (n.d.-b) *Solar photovoltaic technology basics*. Available at: Solar photovoltaic technology basics (Accessed: 19 August 2026).

U.S. Department of Energy (n.d.-c) *Solar integration: inverters and grid services basics*. Available at: Inverters and grid services basics (Accessed: 19 August 2026).

U.S. Department of Energy (n.d.-d) *Solar integration: distributed energy resources and microgrids basics*. Available at: Distributed energy resources and microgrids basics (Accessed: 19 September 2026).

UNFCCC (2015) *Paris Agreement*. Article 2. Available at: Paris Agreement (Accessed: 19 September 2026).

University of Oregon Solar Radiation Monitoring Laboratory (n.d.) *Sun Path Chart Program*. Available at: Sun Path Chart Program.

Wiginton, L.K., Nguyen, H.T. and Pearce, J.M. (2010) 'Quantifying rooftop solar photovoltaic potential for regional renewable energy policy', *Computers, Environment and Urban Systems*, 34(4), pp. 345–357.

Winkler, C., Dabrock, K., Kapustyan, S., Hart, C., Heinrichs, H., Weinand, J.M., Linßen, J. and Stolten, D. (2025) 'High-resolution rooftop photovoltaic potential assessment for a resilient energy system in Ukraine', *Energy Conversion and Management: X*, 28, 101242. doi: 10.1016/j.ecmx.2025.101242.

World Bank Group and Solargis (n.d.) *Global Solar Atlas 2.0* [online dataset]. Available at: Global Solar Atlas (Accessed: 24 September 2026).

Appendix A Monthly PV source values

The tables retain the monthly PVGIS generation values in kWh. Annual totals use the exported annual values, with one decimal shown for presentation; calculations retain full precision. All 108 monthly cells were checked against the source exports.

N–S monthly values

Table A.1 N–S monthly PV generation (kWh). Source: PVGIS exports for the 35° racks, 15° racks and redesigned roof.

Month	**35° racks**	**15° racks**	**Redesigned roof**
January	964.9	1,055.5	1,512.2
February	1,484.4	1,750.7	2,675.3
March	2,537.1	3,242.2	5,266.2
April	3,179.7	4,366.8	7,437.7
May	3,663.4	5,314.9	9,347.1
June	3,770.5	5,623.9	10,046.6
July	3,786.5	5,571.0	9,874.9
August	3,642.6	5,099.6	8,777.9
September	2,987.0	3,877.0	6,357.7
October	2,121.9	2,528.2	3,892.3
November	942.8	1,059.6	1,554.1
December	742.3	784.1	1,087.0
Annual PVGIS	29,823.0	40,273.3	67,828.9

E–W monthly values

Table A.2 E–W monthly PV generation (kWh). Source: PVGIS exports for the 35° racks, 15° racks and redesigned roof.

Month	**35° racks**	**15° racks**	**Redesigned roof**
January	982.9	1,194.3	1,833.2
February	1,512.1	1,981.1	3,040.7
March	2,584.5	3,668.8	5,631.3
April	3,239.1	4,941.4	7,584.5
May	3,731.8	6,014.2	9,231.1
June	3,840.9	6,363.9	9,767.8
July	3,857.2	6,304.0	9,676.0
August	3,710.7	5,770.5	8,857.1
September	3,042.8	4,387.1	6,733.7
October	2,161.5	2,860.8	4,391.1
November	960.4	1,199.0	1,840.3
December	756.1	887.2	1,361.8
Annual PVGIS	30,380.0	45,572.5	69,948.4

SE–NW monthly values

Table A.3 SE–NW monthly PV generation (kWh). Source: PVGIS exports for the 35° racks, 15° racks and redesigned roof.

Month	35° racks	15° racks	Redesigned roof
January	746.4	805.5	1,672.6
February	1,148.3	1,336.1	2,835.1
March	1,962.8	2,474.3	5,352.1
April	2,459.9	3,332.6	7,340.1
May	2,834.1	4,056.1	9,107.1
June	2,917.0	4,291.9	9,668.9
July	2,929.3	4,251.6	9,564.9
August	2,818.0	3,891.8	8,634.0
September	2,310.9	2,958.8	6,402.3
October	1,641.5	1,929.4	4,092.0
November	729.4	808.6	1,684.8
December	574.3	598.4	1,221.4
Annual PVGIS	23,071.9	30,734.9	67,575.2

Appendix B Heat-pump conversion

Hourly heating, cooling and hot-water demand are converted into electricity using the equations in Section 5.3. Heating and hot-water COP follow the relationship developed by Staffell et al. (2012), as reproduced by Thomassen et al. (2024, p. 12). Cooling EER is interpolated between the approximate values from Ounis et al. (2022), listed below. These coefficients vary with hourly outdoor temperature, while the adopted water-supply temperatures remain fixed.

For heating and hot water, when the temperature difference ΔT falls below 15 K, COP is kept at the value calculated for 15 K. COP is never allowed to fall below 1. For temperature differences above 60 K, the same polynomial is extended beyond this range. This extension applies to 2.6% of annual hot-water thermal demand and none of the heating demand.

For cooling, EER is fixed at 5 when ΔT is below 10 K and at 1 when ΔT exceeds 60 K. The lower-temperature limit applies to 0.5% of annual cooling thermal demand. Electricity consumption is calculated by dividing thermal demand by the hourly COP or EER multiplied by the assumed delivery efficiency of 0.91. This efficiency is applied once to account for delivery losses. The calculation represents generic equipment performance; it does not separately calculate defrost cycles, changes caused by equipment switching on and off, or auxiliary pump electricity.

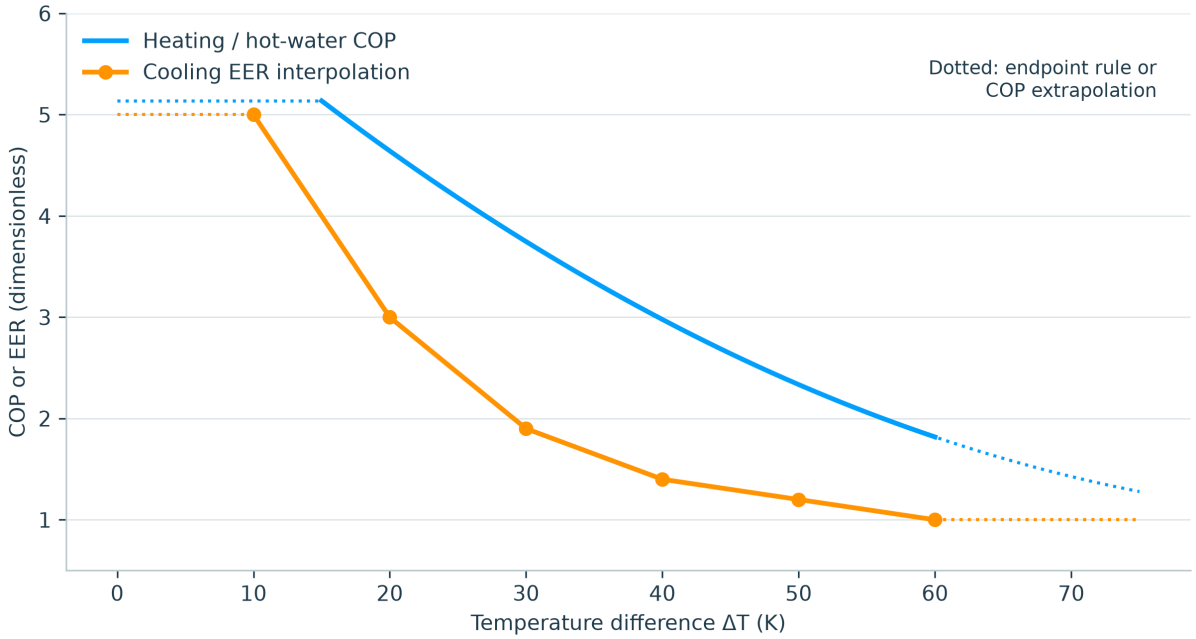

Figure B.1 Temperature-dependent performance before the 0.91 delivery allowance. COP: Staffell et al. (2012), reproduced by Thomassen et al. (2024). EER: approximate values from Ounis et al. (2022). Dotted segments show endpoint rules or extrapolation.

Table B.1 Cooling EER interpolation points.

ΔT (K)	**10**	**20**	**30**	**40**	**50**	**60**
EER	5.0	3.0	1.9	1.4	1.2	1.0

Table B.2 Monthly electricity after conversion (MWh). Rounding may affect displayed sums.

Month	Appliances and cooking	Lighting	Heating	Cooling	Hot water	Total
Jan	3.1	0.6	7.0	0.0	3.0	13.7
Feb	2.8	0.6	4.7	0.0	2.6	10.7
Mar	3.1	0.6	2.5	0.0	2.5	8.7
Apr	3.0	0.6	0.7	0.0	2.0	6.4
May	3.1	0.6	0.1	0.1	1.7	5.6
Jun	3.0	0.6	0.0	1.0	1.4	5.9
Jul	3.1	0.6	0.0	2.0	1.3	7.0
Aug	3.1	0.6	0.0	1.2	1.3	6.2
Sep	3.0	0.6	0.0	0.3	1.5	5.4
Oct	3.1	0.6	0.7	0.0	1.9	6.2
Nov	3.0	0.6	3.5	0.0	2.2	9.2
Dec	3.1	0.6	5.6	0.0	2.7	12.0
Annual	36.0	7.4	24.9	4.7	24.2	97.1

Appendix C Incident radiation legend detail

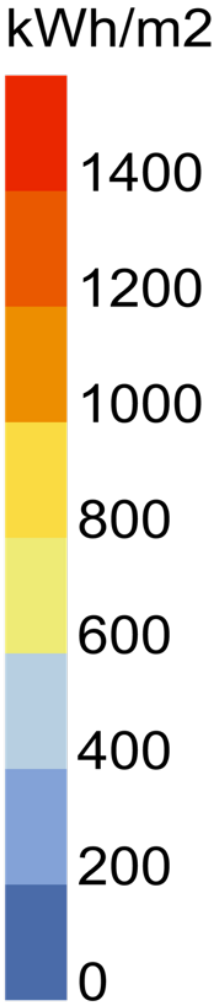

Figure C.1 Common annual incident-radiation legend used for all nine configurations in Figure 4.9, from 0 to 1,400 kWh/m². Source: author's Ladybug export.

All nine configurations use the same fixed legend, ranging from 0 to 1,400 kWh/m² with eight legend segments. These settings are recorded in the Grasshopper definition used for Figure 4.9. The colour scale represents annual incident solar radiation on the analysed geometry and supports comparison of exposure and local shading across the nine configurations.

Appendix D District roof schedules

The schedules retain all 63 roof units used in Chapter 6. IDs correspond to the maps; annual values are PVGIS estimates under the stated roof-layout assumptions.

Schedule D.1 Selected roof geometry and generation

Each ID identifies one assessed roof unit. Axis and PV facing are measured clockwise from true north. T slopes across the width. Usable plan area follows the 0.50 m setback. Panel counts include the common service allowance.

Roof unit	Usable plan m²	Length m	Width m	Axis °	Form	Tilt °	PV facing °	Panels	Capacity kWp	Generation MWh/year
001	810.9	67.9	13.1	68.1	T	12.9	158.1	327	165.1	170.6
003	1,498.5	113.3	14.3	151.2	T	11.8	241.2	618	312.1	306.3
004	842.9	68.7	13.5	68.9	T	12.6	158.9	370	186.9	192.8
006	763.9	68.4	12.3	63.1	T	13.7	153.1	336	169.7	175.3
009	890.1	67.9	14.3	55.0	T	11.8	145.0	363	183.3	186.3
010	834.0	68.5	13.4	67.7	T	12.6	157.7	350	176.8	182.3
012	796.2	68.3	12.8	60.0	T	13.2	150.0	327	165.1	169.7
016	821.2	66.4	13.6	68.8	T	12.5	158.8	356	179.8	185.4
017	828.3	67.7	13.4	65.7	T	12.6	155.7	363	183.3	188.8
020	934.4	73.6	13.9	55.7	T	12.2	145.7	395	199.5	203.2

Roof unit	Usable plan m²	Length m	Width m	Axis °	Form	Tilt °	PV facing °	Panels	Capacity kWp	Generation MWh/year
026	777.1	67.9	12.6	62.8	T	13.4	152.8	327	165.1	170.3
030	1,370.3	110.6	13.5	155.7	T	12.5	245.7	600	303.0	295.6
033	1,449.7	113.2	13.9	119.6	T	12.2	209.6	618	312.1	319.1
034	774.6	66.7	12.8	62.7	T	13.2	152.7	327	165.1	170.2
037	820.2	73.0	12.4	36.0	T	13.6	126.0	355	179.3	179.0
041	843.9	75.5	12.3	54.3	T	13.7	144.3	364	183.8	188.3
042	831.0	74.7	12.3	145.8	T	13.7	235.8	364	183.8	182.9
043	869.3	73.3	13.0	22.2	T	13.0	112.2	355	179.3	174.5
044	889.3	73.6	13.3	51.2	T	12.8	141.2	355	179.3	182.2
048	837.6	72.2	12.8	112.3	T	13.2	202.3	355	179.3	185.4
049	907.6	74.4	13.4	36.7	T	12.6	126.7	400	202.0	201.3
050	901.2	74.8	13.2	54.2	T	12.8	144.2	364	183.8	187.5
052	813.1	73.0	12.3	49.8	T	13.7	139.8	355	179.3	182.7
053	893.5	74.0	13.2	32.0	T	12.8	122.0	364	183.8	181.9
056	970.0	72.9	14.5	26.3	T	11.7	116.3	395	199.5	195.1
060	897.9	73.5	13.4	112.5	T	12.6	202.5	390	197.0	203.0
061	899.5	74.8	13.2	22.9	T	12.8	112.9	364	183.8	179.1
062	833.7	73.9	12.4	50.6	T	13.6	140.6	364	183.8	187.4
063	1,408.2	108.5	14.1	142.4	T	12.0	232.4	592	299.0	297.5
065	868.0	74.3	12.8	40.5	T	13.1	130.5	364	183.8	184.5
066	885.6	69.2	14.0	21.7	T	12.1	111.7	375	189.4	183.9
070	651.6	61.4	11.8	22.6	T	14.3	112.6	284	143.4	140.0

Roof unit	Usable plan m²	Length m	Width m	Axis °	Form	Tilt °	PV facing °	Panels	Capacity kWp	Generation MWh/year
071	853.8	75.0	12.5	38.4	T	13.5	128.4	364	183.8	184.2
074	626.3	59.0	11.8	22.7	T	14.3	112.7	273	137.9	134.6
076	926.1	75.3	13.5	135.3	T	12.5	225.3	407	205.5	207.0
077	880.1	73.9	13.1	36.5	T	12.9	126.5	364	183.8	183.3
080	733.6	62.1	13.0	22.4	T	13.0	112.4	300	151.5	147.5
082	813.8	75.1	12.0	40.8	T	14.0	130.8	349	176.2	177.6
083	676.5	60.3	12.4	21.9	T	13.6	111.9	291	147.0	143.1
086	1,327.6	106.9	13.5	22.1	T	12.5	112.1	580	292.9	284.9
087	798.2	68.4	12.9	22.5	T	13.1	112.5	333	168.2	163.9
091	916.3	96.5	10.6	22.7	T	15.0	112.7	378	190.9	186.6
093	891.9	74.1	13.2	29.3	T	12.8	119.3	364	183.8	181.1
097	840.1	73.1	12.7	36.7	T	13.3	126.7	355	179.3	179.1
098	916.6	73.1	13.7	26.0	T	12.3	116.0	395	199.5	195.3
100	1,263.5	107.8	12.8	127.2	T	13.1	217.2	528	266.6	271.9
102	840.5	76.0	12.2	21.9	T	13.8	111.9	373	188.4	183.5
104	839.9	68.6	13.4	23.0	T	12.6	113.0	370	186.9	182.1
106	641.2	60.4	11.8	22.5	T	14.3	112.5	278	140.4	137.1
107	868.8	75.0	12.8	122.9	T	13.2	212.9	364	183.8	188.4
108	843.2	74.6	12.5	27.7	T	13.5	117.7	364	183.8	180.9
109	699.1	60.1	12.8	22.1	T	13.2	112.1	291	147.0	143.1
110	698.4	60.6	12.7	22.6	T	13.3	112.6	291	147.0	143.3
111	833.8	74.4	12.4	23.1	T	13.6	113.1	364	183.8	179.5

Roof unit	Usable plan m²	Length m	Width m	Axis °	Form	Tilt °	PV facing °	Panels	Capacity kWp	Generation MWh/year
112	627.1	60.9	11.5	22.3	T	14.6	112.3	262	132.3	129.2
117	1,354.3	110.8	13.3	23.1	T	12.7	113.1	546	275.7	268.8
118	761.1	68.1	12.3	22.6	T	13.7	112.6	327	165.1	161.1
119	1,442.6	111.5	14.1	116.2	T	12.0	206.2	605	305.5	313.1
125	1,159.5	85.7	14.8	113.0	T	11.4	203.0	494	249.5	255.4
128	1,394.7	107.4	14.3	22.6	T	11.9	112.6	578	291.9	283.8
132	1,040.5	87.4	13.1	112.5	T	12.9	202.5	427	215.6	222.7
133	1,563.4	123.5	13.9	22.4	T	12.2	112.4	666	336.3	327.2
134	1,502.2	122.0	13.5	22.7	T	12.5	112.7	655	330.8	322.0

Schedule D.2 Annual generation comparison

L slopes along the length; T across the width. Both use the same modules, setbacks, service allowance and PVGIS settings. Counts are whole panels after allowance. Yield is in kWh/kWp/year. * marks an advantage below 1% before rounding.

L retains the 4.93° reference tilt or becomes shallower where its length would exceed a 3 m rise. Alternative aligned grid positions and both panel rotations were checked for each form. T also exceeded an optimistic L estimate using the full bounding rectangle. The comparison establishes the selected form under the stated assumptions; it is not an unrestricted layout optimisation.

Roof unit	L panels	L yield	L MWh/year	T panels	T yield	T MWh/year	Selected	Advantage %
001	327	950.5	157.0	327	1,033.1	170.6	T	8.7
003	618	954.2	297.8	618	981.6	306.3	T	2.9
004	336	950.1	161.2	370	1,031.9	192.8	T	19.6
006	316	952.3	152.0	336	1,033.4	175.3	T	15.4
009	367	955.1	177.0	363	1,016.2	186.3	T	5.2
010	336	950.6	161.3	350	1,031.5	182.3	T	13.0
012	336	953.4	161.8	327	1,027.9	169.7	T	4.9
016	318	950.4	152.6	356	1,031.3	185.4	T	21.5
017	327	951.4	157.1	363	1,029.8	188.8	T	20.2
020	395	953.9	190.3	395	1,018.8	203.2	T	6.8
026	327	952.4	157.3	327	1,031.5	170.3	T	8.3
030	546	955.0	263.3	600	975.5	295.6	T	12.2
033	618	949.0	296.2	618	1,022.6	319.1	T	7.8
034	327	952.6	157.3	327	1,030.6	170.2	T	8.2
037	338	959.2	163.7	355	998.5	179.0	T	9.3
041	349	954.1	168.1	364	1,024.4	188.3	T	12.0

Roof unit	L panels	L yield	L MWh/year	T panels	T yield	T MWh/year	Selected	Advantage %
042	344	959.1	166.6	364	994.9	182.9	T	9.8
043	355	961.6	172.4	355	973.6	174.5	T	1.3
044	355	955.3	171.3	355	1,016.6	182.2	T	6.4
048	355	950.0	170.3	355	1,034.3	185.4	T	8.9
049	364	958.8	176.2	400	996.7	201.3	T	14.2
050	364	954.2	175.4	364	1,020.1	187.5	T	6.9
052	338	955.8	163.1	355	1,018.9	182.7	T	12.0
053	364	959.8	176.4	364	989.8	181.9	T	3.1
056	395	961.1	191.7	395	978.0	195.1	T	1.8
060	355	950.0	170.3	390	1,030.8	203.0	T	19.2
061	364	961.1	176.7	364	974.6	179.1	T	1.4
062	344	955.4	166.0	364	1,019.4	187.4	T	12.9
063	592	953.5	285.1	592	995.2	297.5	T	4.4
065	364	957.9	176.1	364	1,004.0	184.5	T	4.8
066	375	962.8	182.3	375	971.3	183.9	T	0.9*
070	270	965.1	131.6	284	976.5	140.0	T	6.4
071	364	958.3	176.1	364	1,001.9	184.2	T	4.6
074	253	966.0	123.4	273	976.5	134.6	T	9.1
076	364	956.6	175.8	407	1,007.0	207.0	T	17.7
077	364	958.9	176.3	364	997.2	183.3	T	4.0
080	300	964.9	146.2	300	973.9	147.5	T	0.9*
082	349	957.7	168.8	349	1,007.6	177.6	T	5.2
083	278	965.6	135.6	291	974.0	143.1	T	5.6

Roof unit	L panels	L yield	L MWh/year	T panels	T yield	T MWh/year	Selected	Advantage %
086	528	955.7	254.8	580	972.6	284.9	T	11.8
087	336	962.9	163.4	333	974.4	163.9	T	0.3*
091	378	957.0	182.7	378	977.8	186.6	T	2.2
093	364	960.3	176.5	364	985.4	181.1	T	2.6
097	355	959.0	171.9	355	998.9	179.1	T	4.2
098	390	961.1	189.3	395	979.0	195.3	T	3.2
100	528	950.9	253.5	528	1,019.7	271.9	T	7.2
102	355	961.0	172.3	373	974.4	183.5	T	6.5
104	336	962.7	163.4	370	974.4	182.1	T	11.5
106	262	965.5	127.7	278	976.2	137.1	T	7.3
107	364	953.1	175.2	364	1,024.9	188.4	T	7.5
108	344	960.4	166.8	364	984.4	180.9	T	8.5
109	291	965.6	141.9	291	973.7	143.1	T	0.8*
110	291	965.4	141.9	291	974.9	143.3	T	1.0*
111	344	961.2	167.0	364	976.3	179.5	T	7.5
112	262	965.3	127.7	262	976.3	129.2	T	1.1
117	546	955.2	263.4	546	974.7	268.8	T	2.0
118	316	962.9	153.7	327	975.4	161.1	T	4.8
119	605	948.3	289.7	605	1,024.9	313.1	T	8.1
125	494	949.1	236.8	494	1,023.7	255.4	T	7.9
128	578	955.6	278.9	578	972.4	283.8	T	1.8
132	427	948.8	204.6	427	1,032.6	222.7	T	8.8

Roof unit	L panels	L yield	L MWh/year	T panels	T yield	T MWh/year	Selected	Advantage %
133	666	953.9	320.8	666	972.7	327.2	T	2.0
134	595	954.1	286.7	655	973.6	322.0	T	12.3

Appendix E Appliances and cooking

The proposed package serves 30 apartments and 80 residents. One fridge-freezer, dishwasher and washing machine is provided per apartment; laundry is air-dried. Household landlines are excluded, while mobile charging is included with rechargeable devices. The quantities and exclusions are scenario assumptions. Usage values follow Passive House Institute (2023, Table 9, p. 81); manufacturer and EPREL data specify the three large appliances. This is an appliance estimate, not a PHPP certification assessment.

Table E.1 Annual appliance and cooking electricity for the whole building. Calculated results are shown to one decimal; source inputs retain their published precision. Standby is included where specified.

Appliance	Quantity and use assumptions	Source	kWh/year
Fridge-freezer	30 × Bosch KGN39OXBT; 129 kWh/year each.	Bosch (n.d.)	3,870.0
Electric cooking	500 uses/person/year × 0.25 kWh/use × 80 residents.	PHI (2023), Table 9	10,000.0
Dishwasher	30 × Bosch SMV4ECX28E; 14 place settings; 0.543 kWh/eco cycle; standby included.	PHI (2023); European Commission (n.d.-c)	2,541.6
Washing machine	30 × Haier HW80-BP1439N; 8 kg; 0.470 kWh/weighted eco cycle; standby included.	PHI (2023); European Commission (2019; n.d.-d)	2,349.2
Televisions	56 units (0.7/person); 60 W; 4 h/person/day; 0.5 W standby.	PHI (2023), Table 9	7,194.9
Laptops	64 units (0.8/person); 35 W; 5 h/person/day; 0.75 W standby.	PHI (2023), Table 9	5,421.0
Rechargeable devices	80 personal allowances × 0.03 kWh/day.	PHI (2023), Table 9	876.0
Routers	30 units × 0.14 kWh/day.	PHI (2023), Table 9	1,533.0
Microwave/toaster	30 units; 1 use/person/week; 0.25 h/use; 900 W; 0.75 W standby.	PHI (2023), Table 9	1,132.3
Food processor/mixer	30 units; 3 uses/apartment/week; 0.08 h/use; 1,200 W.	PHI (2023), Table 9	449.3

Appliance	Quantity and use assumptions	Source	kWh/year
Vacuum cleaner	30 units; 1 use/apartment/week; 0.5 h/use; 750 W.	PHI (2023), Table 9	585.0
Total appliances and cooking	**1,198.4 kWh/apartment/year; 21.2 kWh/m²/year.**	**Author's calculation**	**35,952.3**

Dishwashing: the PHI workload is 65 cycles per person and year at 12 place settings. Scaling to a 14-place-setting appliance gives 65 × 80 × 12/14 = 4,457.1 cycles/year. Active electricity uses 0.543 kWh/cycle. The 0.5 W standby allowance applies to remaining hours after 4.5 hours per operating cycle. Eco programmes and full loads are assumed.

Laundry: the PHI workload is 57 × 5 kg per person and year, or 22,800.0 kg/year. EU label weights for full, half and quarter loads are 0.379, 0.271 and 0.350 (European Commission, 2019, Annex IV). For the 8 kg washer, the weighted load is 4.816 kg, giving 4,734.2 cycles/year. Active electricity uses 0.470 kWh per weighted cycle. Standby at 0.5 W uses the remaining hours after the label-weighted 3.0658-hour cycle duration. Appliance water heating is already included in both washing-cycle figures.

Television and laptop use is calculated in hours per person, while ownership counts determine standby hours. Weekly uses are multiplied by 52 and daily uses by 365. The remaining small-device categories retain the PHI assumptions. PHI denotes Passive House Institute. The product examples establish energy specifications; they are not procurement commitments.

The 35,952.3 kWh annual allowance is implemented through the existing apartment equipment schedule, equivalent to 5,763.4 full-load hours annually. Dividing this allowance by the schedule hours and the 1,697.0 m² zone area gives a design density of approximately 3.7 W/m²; the simulation uses the unrounded value. The retained aggregate equipment heat-gain split is 50% radiant and 50% convective, with no separate latent or lost fraction. These are simulation assumptions, distinct from the appliance source data. Lighting remains 7,353.6 kWh/year and is not included in the appliance table.

EPREL identifiers are 1961923 for Bosch SMV4ECX28E and 339290 for Haier HW80-BP1439N. The product sheets and PHI criteria were accessed on 22 September 2026. Lighting, space heating, cooling and building domestic hot water remain separate end uses; the appliance total includes only the water heating internal to washing and dishwashing cycles.